

AD-A185 136

IN-SITU CHARACTERIZATION OF THE INTERFACE OF GLASS
REINFORCED COMPOSITES. (U) NATIONAL BUREAU OF STANDARDS
GAITHERSBURG MD POLYMERS DIV F W WANG ET AL. JUN 87

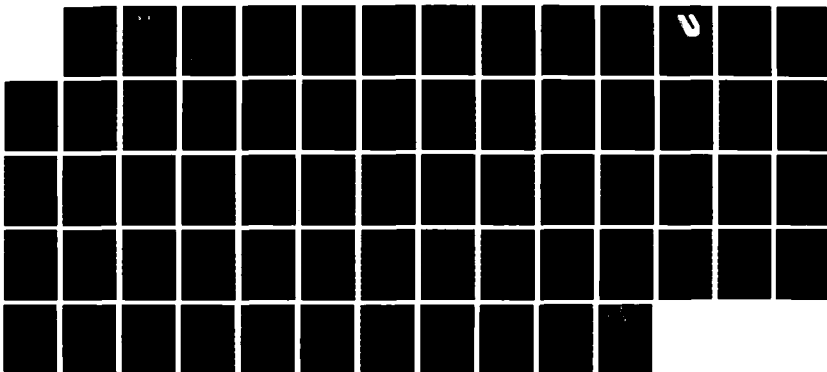
1/1

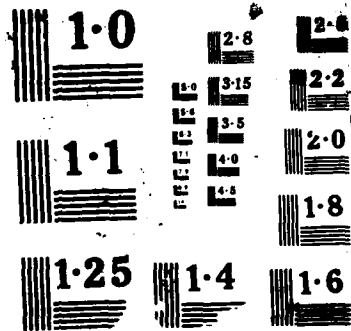
UNCLASSIFIED

NBSIR-87-3581 ARO-21023. 4-MS

F/G 11/4

NL





DTIC FILE COPY

CLASSIFIED
SECURITY CLASSIFICATION

MASTER COPY

FOR REPRODUCTION PURPOSES

DOCUMENTATION PAGE

2

AD-A185 136

1a. REPORT SECURITY CLASSIFICATION
Unclassified

2b. DECLASSIFICATION/DOWNGRADING SCHEDULE
SEP 14 1987

4. PERFORMING ORGANIZATION REPORT NUMBER(S)
D

1b. RESTRICTIVE MARKINGS

3. DISTRIBUTION/AVAILABILITY OF REPORT
Approved for public release; distribution unlimited.

5. MONITORING ORGANIZATION REPORT NUMBER(S)
ARO 21023.4-MS

6a. NAME OF PERFORMING ORGANIZATION
U.S. National Bureau of Standards

6b. OFFICE SYMBOL (if applicable)

7a. NAME OF MONITORING ORGANIZATION
U. S. Army Research Office

6c. ADDRESS (City, State, and ZIP Code)
Inst. for Materials Sci & Eng
Gaithersburg, MD 20899

7b. ADDRESS (City, State, and ZIP Code)
P. O. Box 12211
Research Triangle Park, NC 27709-2211

8a. NAME OF FUNDING/SPONSORING ORGANIZATION
U. S. Army Research Office

8b. OFFICE SYMBOL (if applicable)

9. PROCUREMENT INSTRUMENT IDENTIFICATION NUMBER
MIPR ARO 111-84 ARO 113-85 ARO 145-86

8c. ADDRESS (City, State, and ZIP Code)
P. O. Box 12211
Research Triangle Park, NC 27709-2211

10. SOURCE OF FUNDING NUMBERS

PROGRAM ELEMENT NO	PROJECT NO.	TASK NO.	WORK UNIT ACCESSION NO

11. TITLE (Include Security Classification)
IN-SITU CHARACTERIZATION OF THE INTERFACE OF GLASS REINFORCED COMPOSITES

12. PERSONAL AUTHOR(S)
F. W. Wang and B. M. Fancoini

13a. TYPE OF REPORT
Final

13b. TIME COVERED
FROM 12/25/83 TO 12/24/87

14. DATE OF REPORT (Year, Month, Day)
June 1987

15. PAGE COUNT
58

16. SUPPLEMENTARY NOTATION
The view, opinions and/or findings contained in this report are those of the author(s) and should not be construed as an official Department of the Army position, policy, or decision, unless so designated by other documentation.

17. COSATI CODES

FIELD	GROUP	SUB-GROUP

18. SUBJECT TERMS (Continue on reverse if necessary and identify by block number)
cure monitoring, viscosity, epoxies, fluorescence, optic fibers, remote sensing

19. ABSTRACT (Continue on reverse if necessary and identify by block number)

A technique has been developed to monitor the viscosity of curing epoxies. Fluorescence spectroscopy of viscosity-sensitive organic dyes is used together with optic fibers as a means of delivering the probing light to the measurement site and retrieving the modulated light for detection. The technique is adaptable to remote sensing through the use of optic fibers. The evanescent wave of the guided radiation is used to excite probe molecules lying at the interface between the fiber and surrounding matrix. Therefore, the technique is adaptable to in-situ characterization of the interface of glass reinforced composites.

20. DISTRIBUTION/AVAILABILITY OF ABSTRACT
 UNCLASSIFIED/UNLIMITED SAME AS RPT. DTIC USERS

21. ABSTRACT SECURITY CLASSIFICATION
Unclassified

22a. NAME OF RESPONSIBLE INDIVIDUAL

22b. TELEPHONE (Include Area Code)

22c. OFFICE SYMBOL

NBSIR 87-3581

**IN-SITU CHARACTERIZATION OF THE
INTERFACE OF GLASS REINFORCED
COMPOSITES**

F. W. Wang
B. M. Fanconi

U.S. DEPARTMENT OF COMMERCE
National Bureau of Standards
Institute for Materials Science and Engineering
Polymers Division
Gaithersburg, MD 20899

June 1987

Prepared for:
U.S. Army Research Office
P. O. Box 12211
Research Triangle Park, NC 27709



U.S. DEPARTMENT OF COMMERCE, Malcolm Baldrige, Secretary
NATIONAL BUREAU OF STANDARDS, Ernest Ambler, Director

In-situ Characterization of the Interface of Glass
Reinforced Composites

Final Report

F.W. Wang and B.M. Fanconi

June, 1987

U.S. ARMY RESEARCH OFFICE

MIPR ARO 111-84

Polymers Division
Institute for Materials Science and Engineering
National Bureau of Standards
Gaithersburg, MD 20899

APPROVED FOR PUBLIC RELEASE; DISTRIBUTION UNLIMITED

The view, opinions, and/or findings contained in this report are those of the author(s) and should not be construed as an official Department of the Army position, policy, or decision, unless so designated by other documentation.

TABLE OF CONTENTS

List of Illustrations. ii

List of Tables ii

Introduction 1

Approach 6

 Previous Work 7

 Viscosity-Sensitive Fluorescence. 8

 Excimer Probes. 10

 Use of Dye as Internal Standard 17

 Comparisons with other Techniques 20

Cure Monitoring of Polyimides. 23

 Synthesis of Polyimide. 23

 Results 25

Optic Fiber Sensors. 25

Evanescent Wave Sensors. 27

Experimental Studies 28

Theoretical Considerations 36

References 55

List of Publications Under ARO Sponsorship 58

NOV 2

Accession For	
NTIS	<input checked="" type="checkbox"/>
CRA&I	<input type="checkbox"/>
ERIC	<input type="checkbox"/>
ARR	<input type="checkbox"/>
Unannounced	<input type="checkbox"/>
Justification	
By	
Date	
Availability Codes	
Distribution Statement	
<p>A-1</p>	

LIST OF ILLUSTRATIONS

		<u>Page</u>
1.	Diagram of Cure Monitoring System.	4
2.	Dependence of the Fluorescence Spectrum of 1,3-bis(1-pyrene) propane on Solvent Viscosity.	9
3.	Cure Curve of an Epoxy Monitored with Excimer Dye.	12
4.	Fluorescence and Excitation Spectra of (1-(4-dimethylamino)-6-phenyl-1,3,5 hexatriene).	14
5.	Fluorescence Intensities of Viscosity Sensitive Dye and 9,10-diphenyl anthracence in a Curing Epoxy.	15
6.	Cure Curve of an Epoxy Monitored with Dye Pair of Fig. 5.	16
7.	Comparisons among Cure Monitoring Data for an Epoxy System.	
	a. Fluorescence and Viscometry	18
	b. Fluorescence and Ultrasonics	19
	c. Viscometry and DSC	21
8.	Excitation and Emission Spectra of Poly (amide acid).	24
9.	Optical System for Measurement of Fluorescence using Optical Fiber Probes.	29
10.	Fluorescence Spectrum of Rhodamine-B.	30
11.	Dependence of Fluorescent Light Intensity Collected by Waveguide-Type Optic Fiber on Fiber Length.	31
12.	Dependence of Fluorescent Intensity Collected by Optic Fiber on Solvent Refractive Index.	33
13.	Evanescent Wave Amplitude.	42
14.	Collection Efficiency of Optic Fiber Sensor.	44
15.	Angular Distribution of Radiation from Dipole Source.	50
16.	Comparison of Calculated and Observed Collection Efficiency of Optic Fiber Sensor.	52

LIST OF TABLES

1.	Input Parameters for Modeling Optic Fiber Collection Efficiency.	38
----	--	----

INTRODUCTION

Polymer matrix composite materials are increasingly used in Army applications owing to the advantages of light weight, corrosion resistance and high specific strength and stiffness¹. It is apparent that wider use of these materials to benefit the Army could be made if more rapid processing of higher quality products could be achieved. Current production methods are slow and labor intensive, and there is a demonstrable need to develop on-line methods for process monitoring, in particular with respect to the interfacial regions coupling the strong and brittle reinforcement fibers to the polymer matrix². In-service monitoring of polymer composites is also important, and as in the case of processing, the interfacial region is primarily of interest. In this report, we present results of a research program to develop sensors capable of process monitoring with emphasis on interfacial properties. The sensors are based on optical fibers which become a permanent part of the polymer composite component after processing and which have the added advantage that they may function as performance monitors when the component is placed in service.

Processing of polymer composites differs from that of the more common thermoplastics in two important aspects. First, polymerization of thermosetting resins occurs in the final stages of product manufacture, and second, the presence of reinforcements, frequently at volume ratios greater than 50%, not only introduces inhomogeneities in thermal expansion coefficients, but also leads to large interfacial regions which can have a pronounced effect on resultant properties³. The development of the interface in terms of consolidation of reinforcement plies and fiber wetting becomes an important aspect of processing, and consequently should be probed by the process monitoring sensors.

The interfacial region is also important in the performance of polymer composites. The accumulation of chemical by-products during manufacture at the interface and of environmental contaminants, such as moisture, may be detrimental to the adhesion between the reinforcements and the matrix resin. Moisture accumulation is known to have an adverse effect on the performance of advanced composites of the sort used in aircraft⁴. One aspect of our program addresses the identification of probes that are sensitive to polarity, and hence may be used to monitor moisture uptake in the interfacial region.

Current trends in polymer composite manufacture to more rapid and automated processing are also driving the demand for on-line process sensors and control technologies. In addition, on-line process monitoring techniques would facilitate the introduction of modified or new resin systems. Currently, extensive laboratory studies must be conducted to optimize the cure cycles before modified or new resin systems can be commercialized. With proper on-line monitoring, the amount of laboratory work can be greatly reduced. Thus, process monitoring should lead to more rapid introduction of improved composite materials and optimization of cure cycles as well as facilitate more rapid and automated processing technologies.

Complex chemical and physical processes are associated with the cure of thermosets, such as epoxy resin materials. In the usual cure cycle, the resin initially exists as a viscous liquid that thins as it is warmed to the temperature of cure. The exothermic cross-linking reactions also contribute to the temperature rise. The growing molecular weight of the thermoset matrix eventually controls the viscosity which increases to a value typical of a gel, and in the latter stages of cure to that of a brittle solid⁵. Chemical reactions may also produce by-products of the cross-linking reactions that may

affect processing and use properties.

Of the various changes that occur, the viscosity is perhaps the most important from a processing standpoint as it influences fiber wetting, devolatilization, uniformity of resin distribution, and consolidation of the reinforcement plies. In the processing environment, the resin viscosity initially decreases as the resin temperature rises to that of the autoclave, and then increases as the molecular weight of the cross-link network dominates the viscosity. If the viscosity decreases too much during the autoclave process, an excess of resin will flow out of the product leading to poor adhesion between the reinforcement plies. If, on the other hand, the viscosity remains too high, or increases too rapidly, the flow may be insufficient to achieve good consolidation of the plies. Thus, knowledge of the time dependence of the viscosity during the cure cycle is necessary for proper adjustment of the autoclave temperature and pressure to achieve high quality products. The time intervals during which the polymer composite is held at specific temperature and pressure may be varied to produce high quality products⁶. The key aspect is to have an on-line monitor of viscosity so that the time-temperature-pressure can be adjusted to optimize processing.

Until recently, only dielectric measurements have been exploited for in-situ monitoring of polymer composites cure⁷⁻⁹. Measurements on curing resins have shown that the dielectric response is dominated by ionic conductivity, even though the concentration of ions is very low in these materials¹⁰. The variability in type and concentration of adventitious ions poses problems for quantification of dielectric cure data. Preliminary work has shown that UV-vis absorption and fluorescence spectroscopy can be used to determine the concentration of some reactive species in chemically labeled epoxies¹¹, and

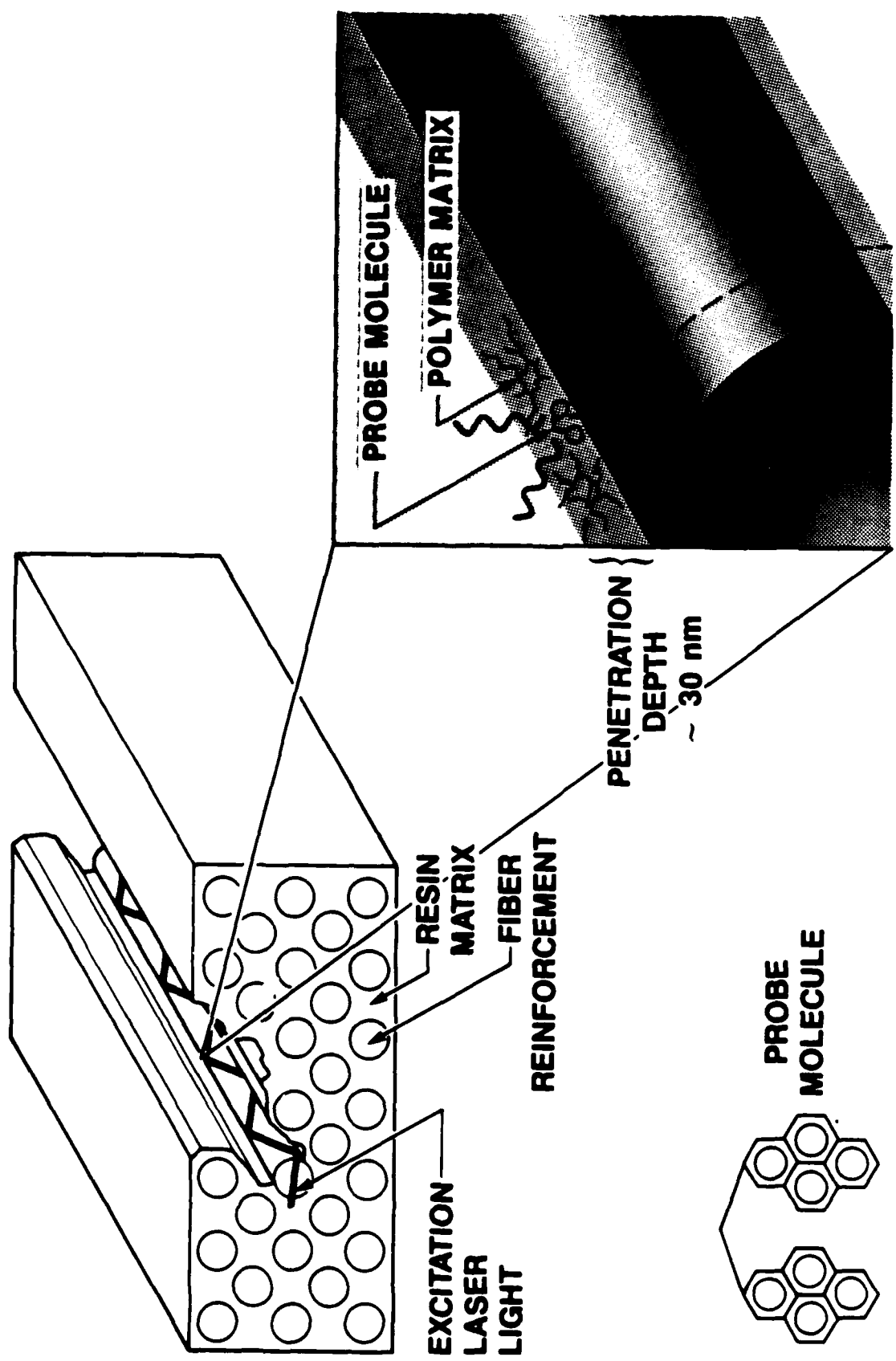


Fig. 1 Monitoring the cure of epoxy resins using viscosity sensitive fluorescence of organic dyes and optic fibers.

that the fluorescence spectra of probe molecules¹² and of specific epoxy systems^{13, 14} are sensitive to local viscosity. The question of the sensitivity of these methods to the interface or of how to make measurements in a remote sensing environment have not been addressed.

On the basis of the above-mentioned considerations, the project reported herein was designed to address measurement of viscosity during processing, albeit in a relative sense, with specificity to the fiber-reinforcement interface. The measurement system was also designed to include the flexibility to monitor chemical changes, at least in selected resin formulations. The major components of the process monitoring approach developed in this project are fluorescent probes in the form of low molecular weight organic dyes that exhibit sensitivity to microviscosity and optic fibers as remote sensors. The application of the method is illustrated in figure 1. Laser light is propagated through an optic fiber imbedded in the composite; probe molecules lying near the optic fiber interface are excited by the evanescent wave of the propagated light; fluorescence from the probe molecules is trapped by the fiber and observed at the end of the fiber.

The fluorescence spectra of organic molecules may be sensitive to the chemical environment at the molecular site as well as to microviscosity¹⁵. In addition, the high quantum yields obtainable with many dyes, laser sources capable of delivering high power in narrow frequency intervals, and sophisticated spectroscopic equipment capable of detection and differentiation on exceedingly low concentrations of dye molecules make the approach viable. In the course of this project, several dye systems have been identified for monitoring viscosity during processing; and detailed investigations have been conducted to demonstrate their application to epoxy resin systems¹⁶⁻¹⁸. In

addition, fluorescence spectra of polyimides have been shown to be sensitive to the chemical environment¹⁸.

For neat resins, conventional fluorimetry has been used to measure the intensities of viscosity probes. This method is generally limited to the surface of a reinforced specimen, particularly for opaque samples. To probe the interior of a specimen, optic fiber sensors have been investigated as a means of transmitting the excitation light to the measurement site and for collecting and transmitting a portion of the fluorescence light to the detector. Optic fibers have the advantage that they can be selectively placed in the specimen to develop an image of the viscosity profile across the specimen. This is particularly important for thick specimens in which a significant temperature gradient between exterior and interior regions may result in non-uniform cross-linking.

The combination of fluorescence probes and optic fiber sensors shows promise as a useful method to monitor the viscosity of a curing matrix resin on-line. Both experimental and theoretical studies have been conducted to determine the optimal conditions for use of optic fibers in viscosity monitoring and for interrogation of the interface region. In the latter use, the interface is between the optical waveguide and the surrounding medium. Since the waveguides are constructed of glass the immediate application is to glass reinforced composites where the reinforcements themselves may serve as the optic fibers.

APPROACH

The approach adopted in this work combines fluorescence probes that exhibit sensitivity to medium viscosity, or the chemical environment, with optic fibers as a means of transmitting the excitation light to the interior of

a composite part as well as for conducting a portion of the modulated light to the detector for analysis.

Previous Work

Sung et al ^{11, 19} used diaminoazobenzene (DAA) as a probe molecule to mimic the reactivity of the cure agent diamino diphenylsulfone. The probe molecules used in our work do not participate in the cross-linking chemistry whereas DAA is a tetrafunctional amine whose UV-VIS absorption and fluorescence spectra are sensitive to the replacement of amine hydrogens by functional groups as occurs during cure. The spectroscopic measurements using DAA track the chemistry of the probe which may or may not be indicative of the cure agent. Also, this probe is restricted to very specific epoxy systems. The absorption technique is limited also by the necessity of relatively high probe concentrations, >.1%, and lack of sensitivity after vitrification. Sung and co-workers have used the fluorescence of DAA as a probe of the cross-linking chemistry¹¹. Comparisons with the fluorescence yields of model compounds have shown that the fluorescence sensitivity of DAA probes reflects the amine functionality rather than viscosity¹¹. The fluorescence of the DAA probe does exhibit changes beyond vitrification, but is limited by the lack of an internal standard.

Other investigators have attempted to use fluorescence associated with certain types of epoxy resins as a means of process monitoring¹³. This approach was discarded early in our work because the approach could not be generalized to other epoxy systems. It has been observed in the course of our work that the band shape and frequency maximum of epoxy fluorescence changes with excitation frequency, source of the epoxy, and state of cure. It is likely that most of this fluorescence signal does not arise from the diglycidil

ether of bisphenol-A, or from epoxy-type intermediaries in the polymerization. If a significant portion of the intensity arose from an impurity, as appears likely, then the spectral response should vary from batch-to-batch as we have observed. For these reasons cure monitoring of epoxies by fluorescence spectroscopy is best accomplished by the intentional addition of a fluorescence probe with a well-defined spectral response. Cure monitoring of polyimides by naturally occurring fluorescence has been demonstrated in our work.

Viscosity-Sensitive Fluorescence

Fluorescence probes that were identified for specificity to the microviscosity fall into two classes, one being the excimer type that has the added advantage of self-calibration, and the second type combining a viscosity sensitive dye with an insensitive dye, the latter of which served as an internal standard¹⁷.

The sensitivity of the fluorescence spectra of some organic dye molecules to viscosity stems from the competition between radiative and non-radiative processes for de-excitation of the electronically excited states²⁰. As the solvent viscosity increases, the degrees of motion of the solute dye molecules are affected to the extent that the probability of large scale movement is diminished. For example, translational modes and rotational modes of a probe molecule are converted into internal modes when the molecule is trapped in a highly viscous medium. Inhibiting molecular mobility reduces the probability of non-radiative decay of the electronic excitation, and fluorescence is enhanced. There are molecules, however, for which the reverse is true, that is the fluorescence intensity of some bands diminishes with decreasing mobility rather than increasing. The latter situation occurs in excimer-forming dyes in

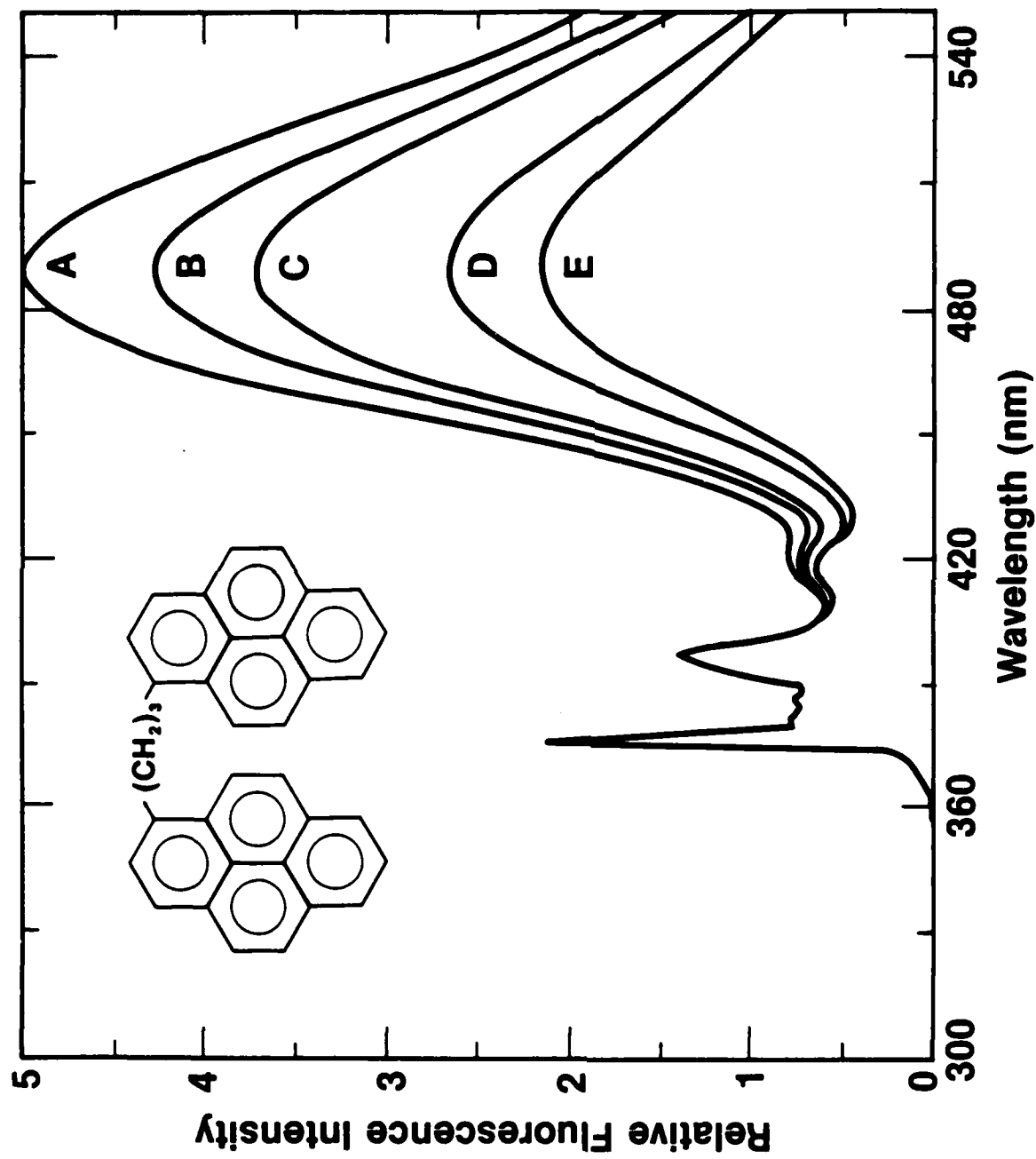


Fig. 2 Dependence of the fluorescence spectrum of 1,3-bis(1-pyrene) propane on solvent viscosity. All spectra are normalized to constant monomer intensity. The solvent viscosity progressively increases from A to E: A, 0.44 cp; B, 0.91 cp; C, 1.36 cp; D, 2.81 cp; E, 4.0 cp.

which mobility enhances the formation of excited electronic state complexes which fluoresce at different wavelengths than the normal emission²¹.

Excimer Probes

One of the two types of probe molecules investigated was excimer-forming. An example is the molecule 1,3-bis-(1-pyrene) propane the structure of which is shown in figure 2. This molecule contains two pyrene rings, the chromophores involved in the electronic excitation, attached to either end of a propane linkage. When the molecule is excited into the excited electronic states of the pyrene group the excitation can follow one of three pathways to de-excitation. One involves non-radiative decay through coupling of the electronic motion to nuclear motions (molecular vibrations, rotations, and translations), another process results in the return to the ground state with emission of light (fluorescence) after a period of time termed the lifetime of the pyrene excited electronic state, and the third pathway involves creation of a new electronic state (excimer state) in which the excitation is shared by both pyrene groups. The relative probabilities of these three processes determine the course of de-excitation. Fluorescence from the excited state of the single pyrene chromophore takes place approximately 100ns after excitation, the lifetime of its excited state, provided that de-excitation has not occurred through the other mechanisms. The probability of non-radiative decay is affected by the strength of the coupling between the electronic and nuclear motions^{22, 23}. The nuclear motions can be affected by the local viscosity of the medium which surrounds the molecule as discussed previously. The probability of the third process, the formation of an excimer state, depends on the relative arrangement of the two pyrene groups. Configurations which maximize overlap of the π -electrons of the two pyrene groups have a high

probability of excimer formation, whereas other conformations have low probability. Maximum overlap occurs when the two pyrene groups adopt a sandwich configuration, that is, the planes of the pyrene rings are face-to-face. Both the inter-chromophore distance and the relative orientation of the two pyrene rings affect the probability²¹.

Internal rotations about the propane segment of 1,3-bis(1-pyrene) propane allow conformations such as the sandwich conformation. An electronically excited molecule undergoes transitions among the various conformations with transition probabilities proportional to the conformational energy barriers. If during the 100ns lifetime of the pyrene excited state, the molecule adopts the sandwich conformation, there is a high probability for excimer formation and fluorescence occurs at longer wavelengths. The conformational energy barriers are dependent on the solvent viscosity which gives the dependence of excimer fluorescence intensity on medium viscosity. An example of the viscosity dependence of excimer fluorescence is given in figure 2 in which fluorescence spectra of 1,3-bis(1-pyrene)propane in solvents having viscosities in the range 0.44 to 4cp are shown. Two fluorescence bands are evident, one from a singly-excited pyrene group(monomer), and the longer wavelength band from the excimer state(dimer). As the solvent viscosity increases, the relative intensity of the excimer emission to the monomer fluorescence decreases or alternately, the ratio of the monomer to excimer fluorescence increases linearly with viscosity.

An advantage of excimer forming dyes for viscosity monitoring is that the monomer fluorescence intensity may be used as an internal standard. The monomer and excimer fluorescence wavelengths are sufficiently well-separated to permit independent intensity measurements. A number of factors, characteristic

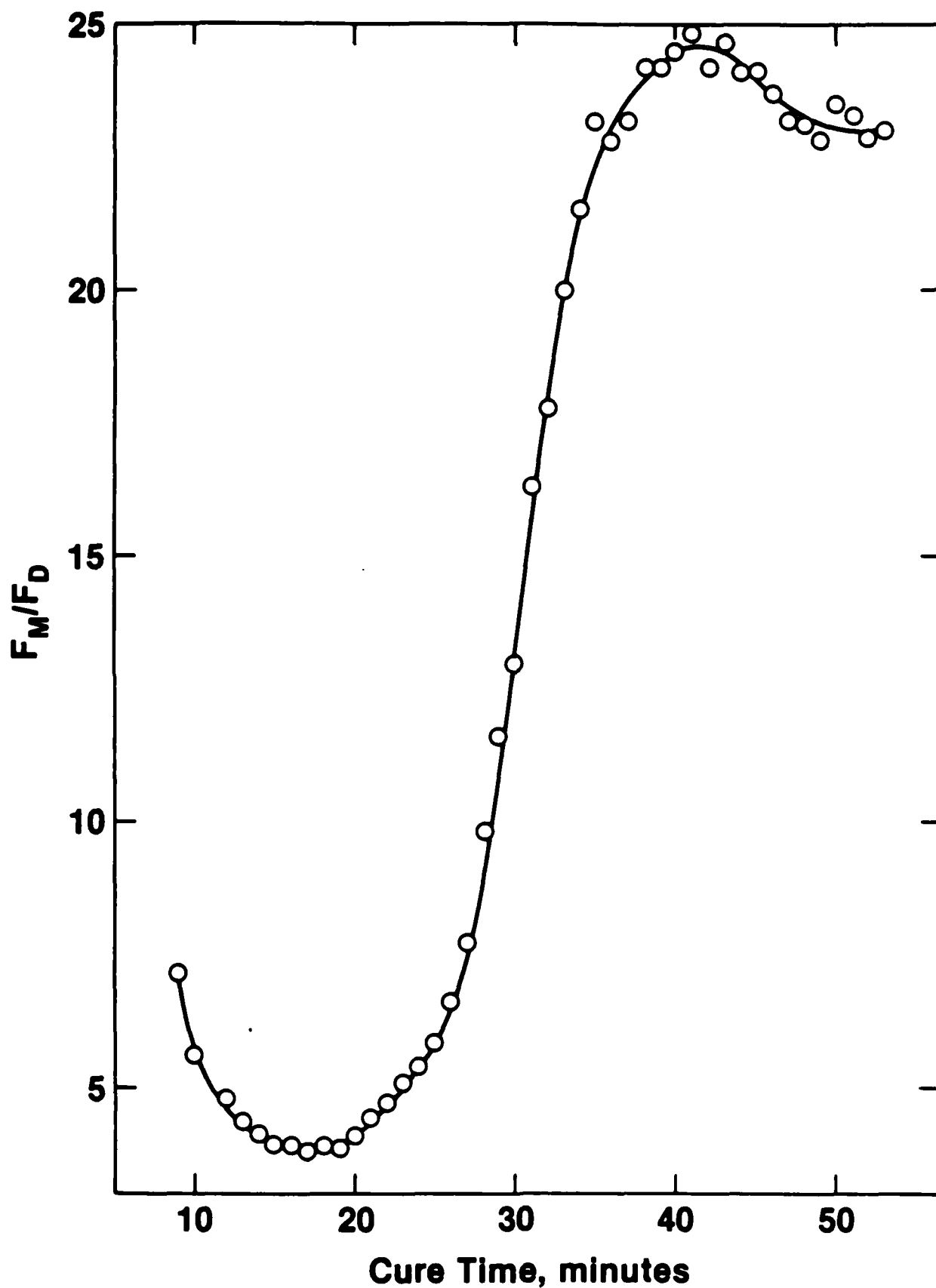


Fig. 3

The cure curve of an epoxy system [EPON 828 cured with 4,4'-methylene-bis(cyclohexamine)] monitored by the fluorescence ratio of the excimer dye, 1,3-bis(1-pyrene) propane.

of both the sample and measurement system, may change during the course of cure. For example, the refractive index of the resin may change, or inhomogeneities may affect the emission intensity. For these reasons, it is highly desirable to have an independent measure of the efficiency of the fluorescence excitation and detection system. The monomer emission of an excimer forming molecule serves this purpose, as long as the active probe concentration does not change as cure proceeds.

We have applied the excimer fluorescence technique to monitor the viscosity change during the cure of an epoxy resin. A trace amount of 1,3-bis-(1-pyrene)propane was dissolved in a stoichiometric mixture of Epon 828¹ (diglycidil ether of bisphenol-A and 4,4'-methylene-bis-(cyclohexylamine)). The intensity ratio, F_m/F_d , where F_m and F_d are the fluorescence intensities of the pyrene monomer and pyrene-excimer (dimer) fluorescence, respectively, was measured as a function of time after the mixture was heated to 60 C. The measured values of the intensity ratio, figure 3, successfully indicated the initial decrease of the resin viscosity due to heating and exothermic reactions, and the subsequent increase of the resin viscosity due to polymerization. The cure curve, figure 3, also shows a drop in the fluorescence ratio at a cure time of 40 minutes. We believe this drop indicated that photochemical reactions were occurring and became appreciable

¹ Certain commercial materials and equipment are identified in this paper in order to specify adequately the experimental procedure. In no case does such identification imply recommendation or endorsement by the National Bureau of Standards, nor does it imply necessarily the best available for the purpose.

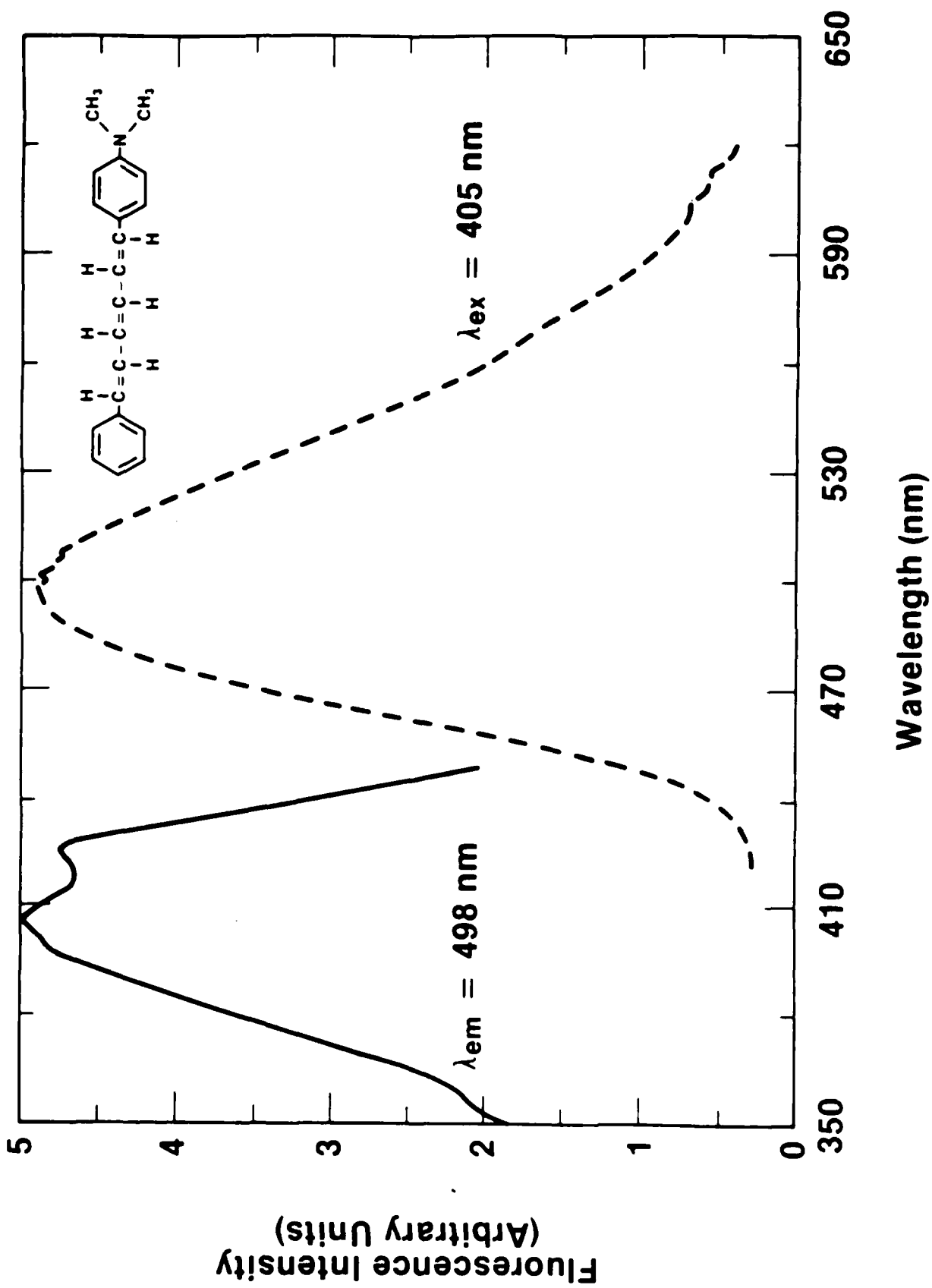


Fig. 4 The fluorescence (dashed curve) and excitation (solid curve) spectra of the viscosity sensitive dye (1-(4-dimethylamino)-6-phenyl-1,3,5-hexatriene), DMA-DPH, in solution.

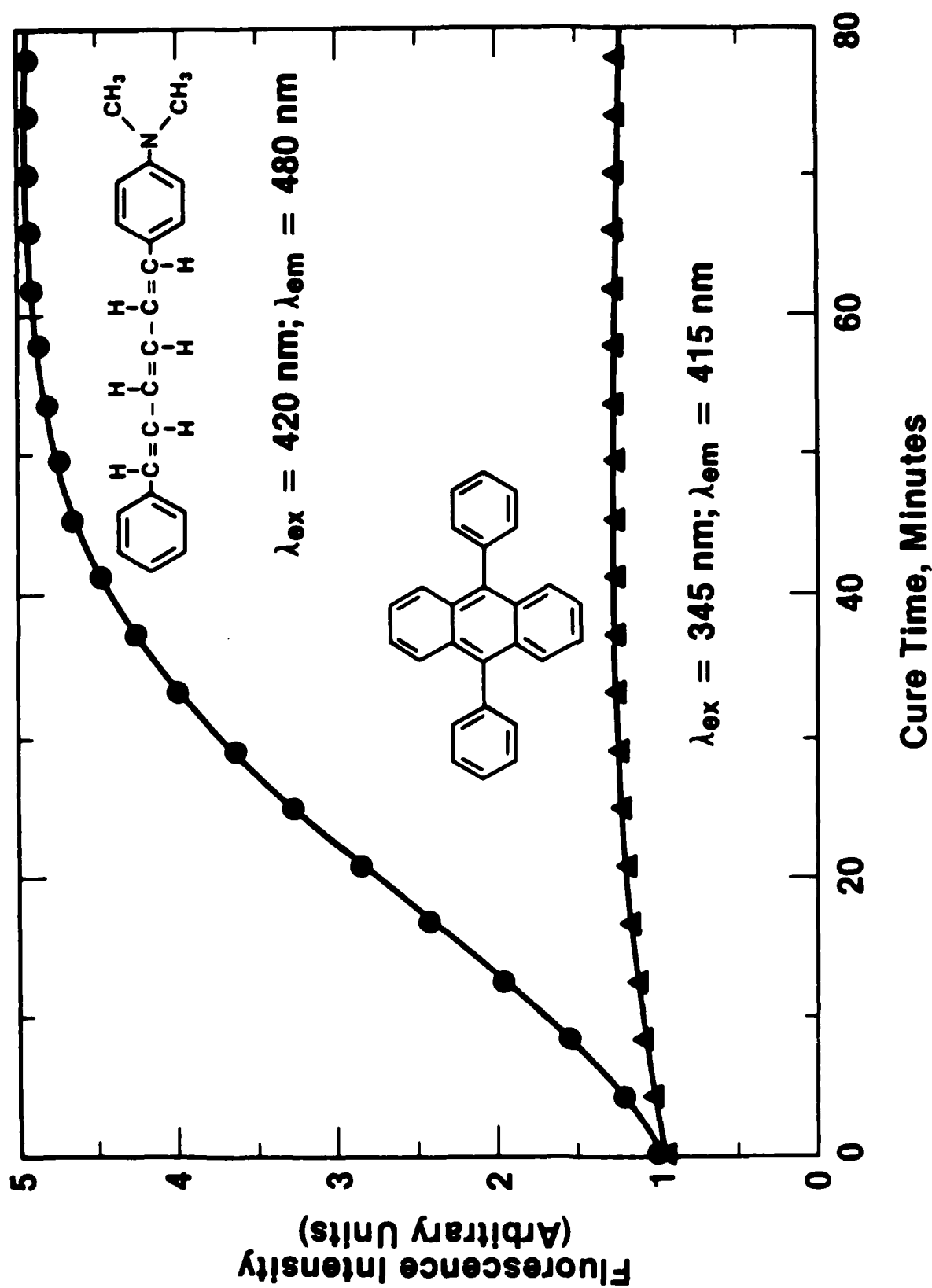


Fig. 5 The fluorescence intensity of DPA-DPH, filled circles, and 9,10 diphenyl anthracene, DPA, filled triangles, in an epoxy system, DER 332 cured with 4,4' methylene-bis-(cyclohexylamine), BPAOM, as a function of cure time.

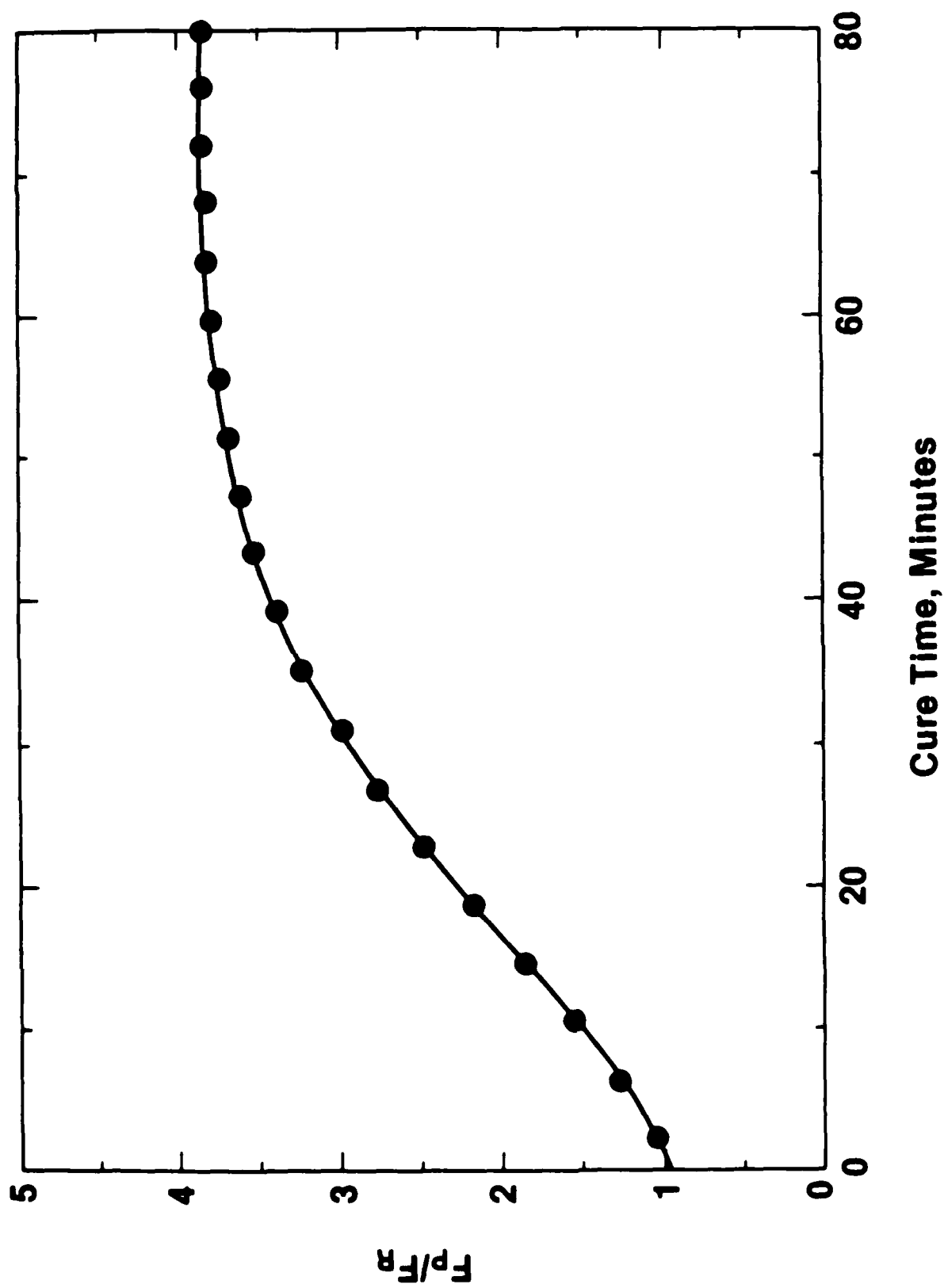


Fig. 6 The cure curve of the epoxy system DER 332 cured with BPAOM monitored with the dye pair DMA-DPH/DPA.

when the resin viscosity was such that probe molecules no longer diffused in and out of the sampling volume. For this reason we have examined other dye molecules for use as viscosity probes.

Use of Dye as Internal Standard

The selection of suitable probe molecules is governed by the following considerations: (1), sensitivity of the fluorescence intensity over a wide range of microviscosity, (2), chemical stability in the cure environment (chemical reactions and photochemistry), (3), excitation and fluorescence frequencies, (4), solubility in the epoxy resin, and (5), internal intensity standard. As stated above, the excimer-type dye satisfies 3-5, but is photosensitive which affects its suitability to monitor the latter stages of cure. Investigations to date have indicated that the optimal probe system is a combination of two dyes. One dye of the pair, eg DMA-DPH, displays fluorescence intensity sensitivity to microviscosity while the other, 9,10-diphenylanthracene, has a fluorescence intensity that is essentially independent of viscosity. The two dyes emit at different frequencies, so that in the course of cure monitoring the luminescence from both can be independently determined. The excitation and emission spectra of the viscosity sensitive molecule we have selected are shown in figure 4. The dependence of their emission intensity on viscosity as measured during the cure of an epoxy resin is shown in figure 5, and the ratioed intensity versus cure time is given in figure 6. In the case of the cure curve, figure 6, the initial time, $t=0$, corresponded to when the resin temperature equaled the temperature of cure and for this reason, the dip in the ratio at early times, corresponding to the rise in resin temperature to that of cure, is missing.

EPOXY 332/BPACM

CURED AT 45 C

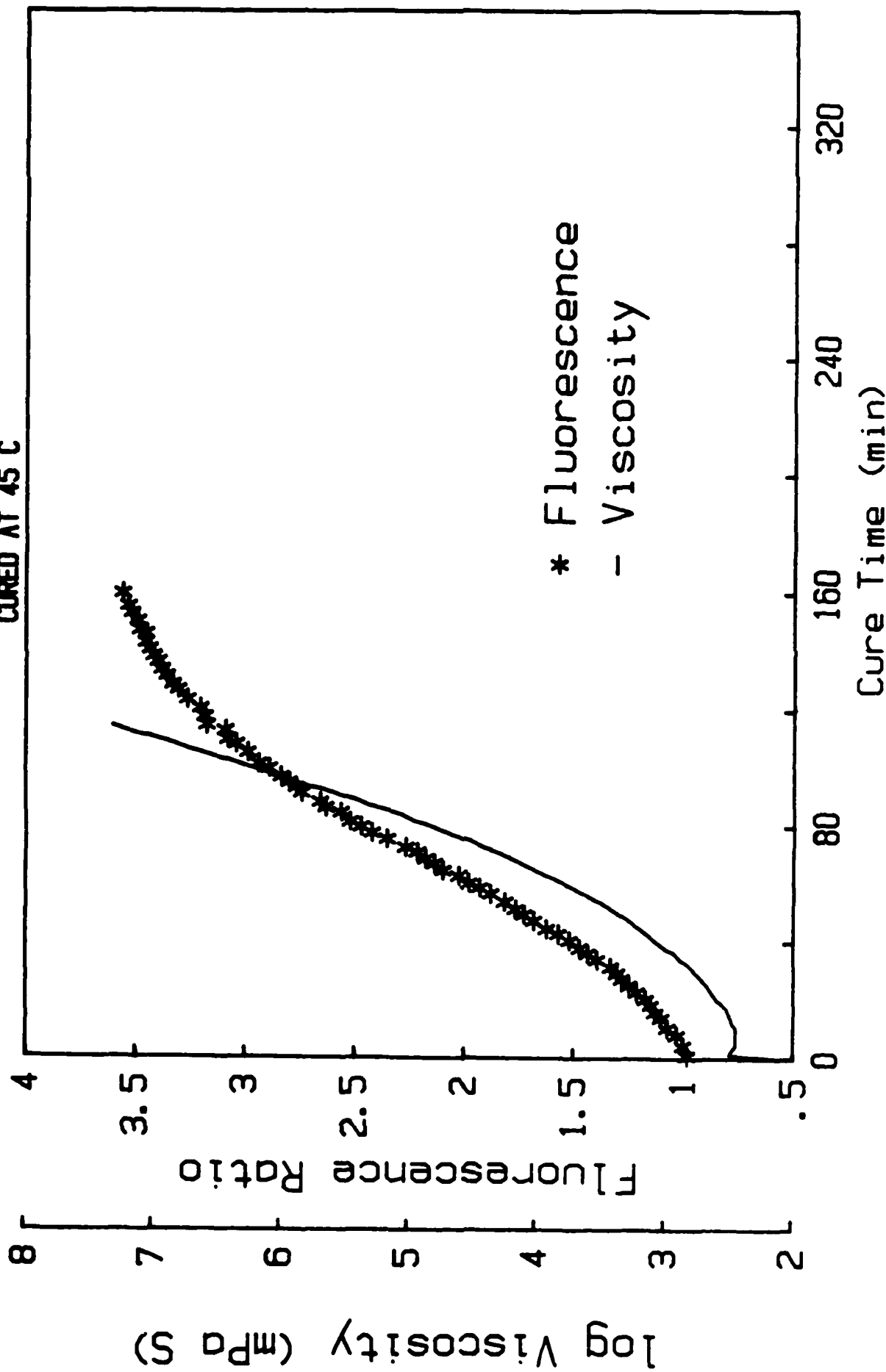


Fig. 7a Comparisons among cure monitoring data for the epoxy resin DER 332/BPACM at 45°C.
a. viscosity and fluorescence data

EPOXY 332/BPACM

CURED AT 45 C

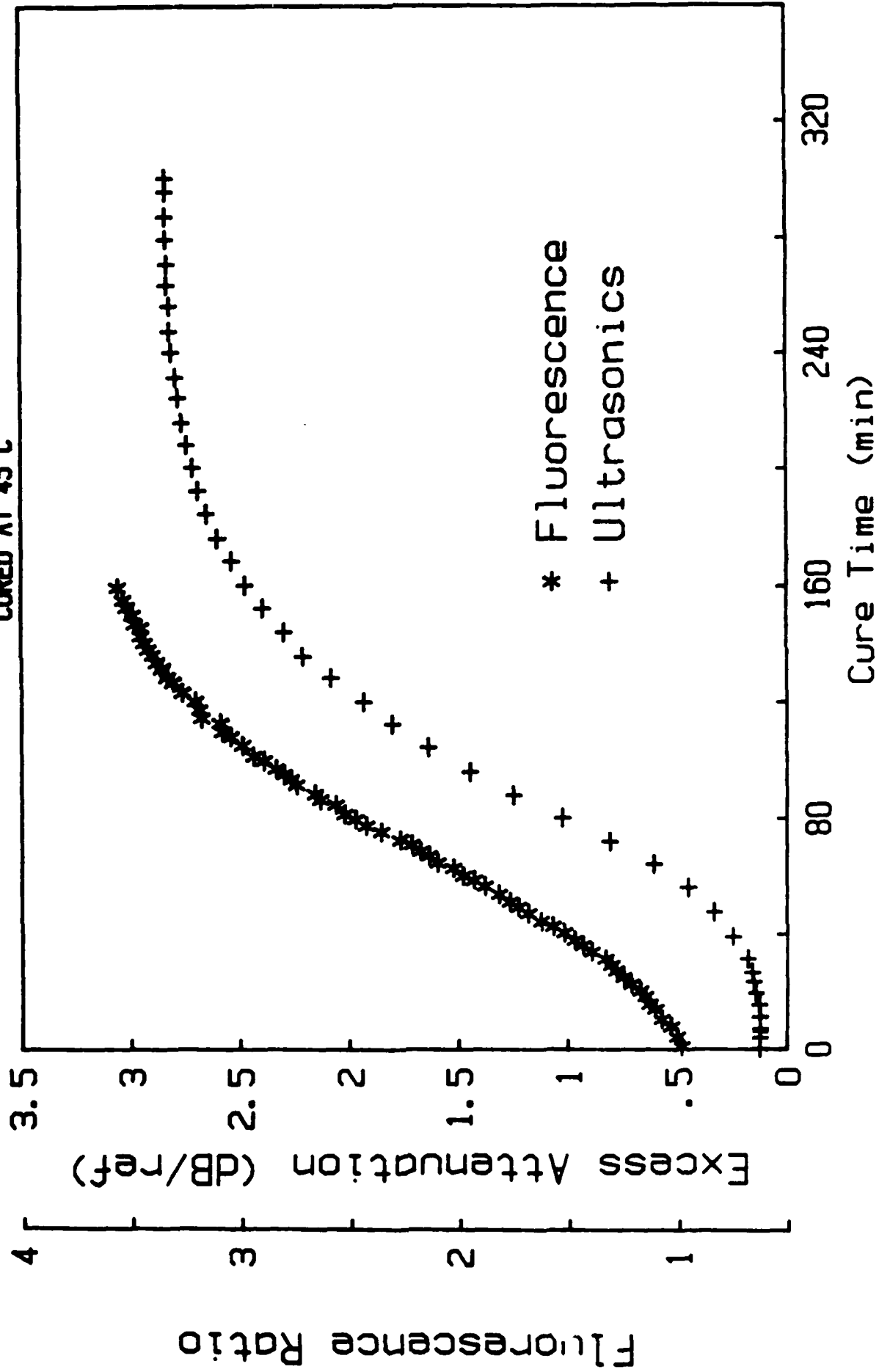


Fig. 7b Comparisons among cure monitoring data for the epoxy resin DER 532 / BPACM at 45°C.
b. ultrasonics and fluorescence data

Comparisons with Other Techniques

The cure curve of figure 6 has been compared to those generated by other experimental techniques and these comparisons are shown in figure 7. In figure 7a, the fluorescence cure curve is compared to that obtained from viscometry. The viscometric data were determined with an automated concentric cylinder viscometer utilizing shear rates between $50s^{-1}$ and $.02s^{-1}$. The departure of the two curves at longer cure times may not be significant because the viscometric data may not be accurate over the entire cure for the following reasons. The measured viscosity is a function of the shear rate, particularly at times corresponding to the rapid rise in viscosity. As the sample approaches gelation, the high stresses involved and the rapid changes in the sample limit the measurement to low shear rates, and thus the shear rate dependence cannot be measured. Moreover, it is difficult to assure that steady state flow is achieved, and thus the data may be only a qualitative measure of viscosity at the highest values. For this reason, the departure between the fluorescence measurement and viscometry at the latter stages of cure does not necessarily indicate a lack of sensitivity on the part of the fluorescence probe.

Figure 7b compares the fluorescence cure curve to that obtained in an ultrasonics measurement of the shear mechanical properties²⁴. The ultrasonic wave propagation technique uses either a quartz plate or rod that is coated or placed in contact with the sample.²⁵ The data presented in figure 7b were obtained with the rod geometry. In this system, a shear wave is generated at one end of the rod and is monitored by a transducer at the end opposite to that placed in contact with the sample. By measuring the reflection coefficient at the coated end (the attenuation

EPOXY 332/BPACM

CURED AT 45 C

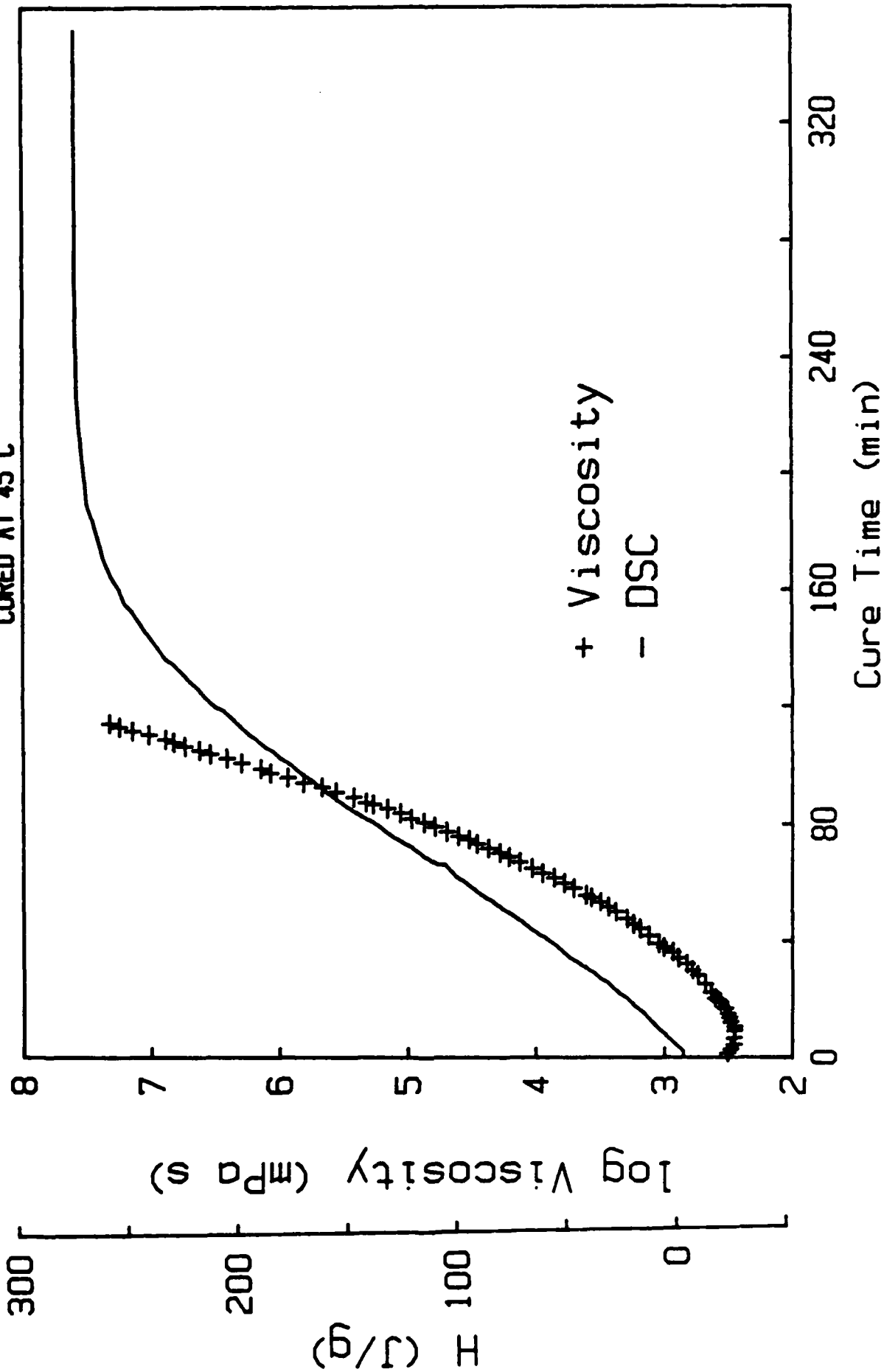


Fig. 7c Comparisons among cure monitoring data for the epoxy resin DIER 332/BPACM at 45°C.
c. DSC and viscosity data

and phase shift of the reflected wave), the mechanical properties of the sample can be determined. Since the attenuation of shear motion is very high until the sample becomes rigid, the measurement is independent of sample thickness. The ultrasonics shear wave method provides a direct measure of the dynamic shear storage (elastic) and loss (viscous) moduli. If desired, the absolute values of these materials properties can be measured and followed during cure. Often, however, it is the relative changes that are of prime interest, and in this case the measurement of the amplitude attenuation coefficient (loss in wave amplitude) per reflection can be used. As the sample cures the attenuation increases markedly but eventually levels off as the cure approaches completion.

The shape of the ultrasonics and fluorescence cure curves are very similar and can be superimposed if shifted along the cure time axis. It has not been determined if there is some inherent difference in the data of the two techniques as relates to viscosity, or if the offset merely reflects a difference in the initial measurement time. Both sets of data were obtained on epoxy resin from the same batch.

The third comparison, figure 7c, is between the fluorescence data and heat evolution measurements. The latter were made by differential scanning calorimetry which measures the heat evolved during the cross-linking reaction. Excellent agreement is found between these two measurements. It is concluded from comparisons between the fluorescence cure curve and those of more traditional techniques of cure and viscosity monitoring that the fluorescence method does provide a reasonable measure of the degree of cure and of the viscosity during epoxy cure.

We conclude from the foregoing that we have demonstrated that

fluorescence probes are effective polymer matrix cure monitors. The fluorescence probes have the added advantage, as will be discussed below, of being adaptable to remote sensing.

CURE MONITORING OF POLYIMIDES

Preliminary work on polyimides has shown that the natural fluorescence from species generated by the cure chemistry can be used as a measure of the degree of cure.

Synthesis of Polyimide

The polyimide was prepared from 2,2-bis(3,4-dicarboxyphenyl) hexafluoropropane dianhydride (American Hoechst 6F)¹ and 2,2-bis[4(4-aminophenoxy)phenyl] hexafluoropropane (Morton Thiokol 4BDAF).

Both 6F and 4BDAF are soluble in dry glyme at 25°C. 4BDAF (0.5g, 9.6×10^{-4} mol) was dissolved in 3 ml of dry glyme at 25°C with stirring in a 25 ml glass-stoppered flask. When dissolution was completed (usually within 3 minutes), 0.42g (9.6×10^{-4} mol) of solid 6F in small portions (0.1g each) was added to the solution of 4BDAF at 25°C. Within 5 minutes after the 6F was added, stirring was impeded by the increased solution viscosity. After 15 minutes of manually swirling the contents, the solution viscosity decreased sufficiently to allow normal stirring to proceed. The reaction was stopped after 44 hours at 25°C. This solution (26% solids) of the poly(amide acid) in glyme was used to prepare films for fluorescence spectroscopy as described below.

A few drops of the poly(amide acid) solution were spread on a clear quartz slide by drawing a wedge of the solution beneath another clean slide. Room temperature solvent evaporation and all heat treatments were carried out in air. The film was cured for 0.5 hour at each of seven temperatures ranging

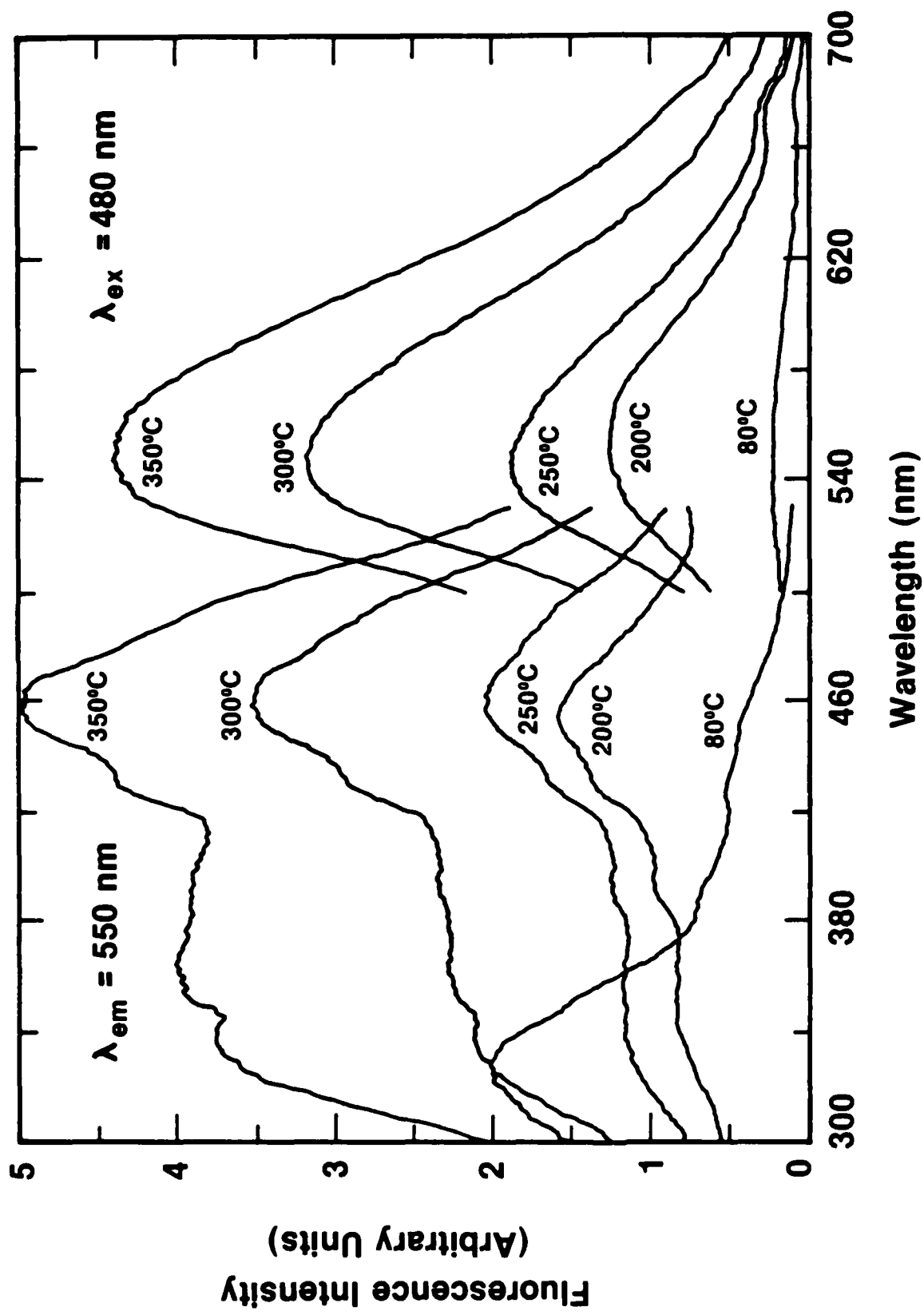


Fig. 8 Excitation and emission spectra of poly(amide acid) after heat treatments.

from 80° to 350°C, with oven warmup and cooling down times of up to 0.5 hour each. Front surface fluorescence from the same film region was measured at room temperature after each heat treatment. Film thickness averaged 13 μ m.

Results

Figure 8 shows the uncorrected excitation and emission spectra of a film of the poly(amide acid) after thermal treatment in an air filled oven for 30 minutes at each of the temperatures ranging from 80°C to 350°C. The excitation and the emission wavelengths were 480 nm and 550 nm, respectively. The fluorescence intensity at 550 nm increased steadily when the cure temperature was raised from 80°C to 350°C. The uncorrected excitation spectra were more complex. A band at 460 nm appeared at the expense of the one at 330 nm after the second heating. However, the intensity of the band at 330 nm relative to the one at 460 nm increased steadily with additional thermal treatments. In any event, the formation of this polyimide polymer can be readily monitored in-situ by fluorescence spectroscopy.

OPTIC FIBER SENSORS

Conventional fluorimetry can be used to monitor the fluorescence of probe molecules in the processing environment, particularly if the manufactured part is transparent or if surface measurements suffice. Indeed, there have been reports of its use in the manufacture of circuit boards²⁶. For general applications in the autoclave environment, or for measurements of cure in the interior of a composite part, it is necessary to use optic fibers as a means of bringing the excitation light to the sampling volume and for transmitting a portion of the modulated radiation to the detector.

Several optic fiber probes specifically designed for fluorescence detection are available commercially, including devices that may be suitable

for use in an autoclave under certain conditions. A common aspect of commercial devices is distal sensor, that is, sample illumination, and in some designs the collection of modulated light, occur at the end of the optic fiber²⁷. The distal end of the optic fiber may have an optic element, such as a lens, incorporated into it. With this sensor design, the material under inspection is situated in a small volume located at the end of the optic fiber. The dimensions of the volume of material interrogated in such sensor designs depend on the numerical aperture and diameter of the fiber, as well as the optic element incorporated into it, if any.

Another type of optic fiber sensor uses the evanescent wave to excite the fluorescence^{24, 28-30}. The volume element, termed the evanescent volume, is rather different from that sensed by the distal-type of optic fiber probe. In the evanescent-type design, the material surrounding the optic fiber to a depth ranging from 30-100nm is measured by the fluorescence technique. Both optic fiber probe designs make use of the guided waves to transmit the radiation to the point of measurement as well as to guide modulated radiation to the detection system. No commercial sensors based on the evanescent wave excitation are currently available, although the design offers advantages in characterization of interfaces and through-specimen sampling. By using an array of waveguide-type sensors, an image of the state-of-cure as a function of cure time of a thick and complex composite part can be made. There are technical difficulties with evanescent-type sensors that must be resolved before this design becomes commercially viable. Our work on optic fiber sensors has explored the potential of the evanescent-type to monitor the fluorescence of probe molecules.

EVANESCENT WAVE SENSORS

In the evanescent-type sensor, the fluorescence is excited by evanescent waves. The evanescent wave arises from total internal reflection at the waveguide-medium interface³¹. As long as the refractive index of the surrounding medium is less than that of the fiber, there will be an angle of incidence at the waveguide-medium interface beyond which light is totally reflected. That angle, termed the critical angle, is given by

$$\theta = \sin^{-1}(n_m/n_g) \quad [1]$$

where n_g is the refractive index of the fiber, n_m is that of the medium and θ is the angle that the ray incident at the fiber-medium interface makes with the surface normal. The salient feature of optic waveguides is that the electric field amplitude of a totally reflected ray does not vanish at the waveguide interface but penetrates a short distance into the surrounding medium of lower refractive index. The electric field in the lower refractive index medium is termed the evanescent wave and its magnitude at a distance z into the medium is proportional to $\exp(-z/d)$, where d is given by

$$d = \lambda/2\pi n_g [\sin(\theta) - (n_m/n_g)^2]^{1/2} \quad [2]$$

In this equation, λ is the wavelength of light in vacuum, θ is the angle of incidence and n_m , n_g are as defined previously. The distance d is referred to as the penetration depth and equals the distance at which the evanescent wave magnitude decreases to $1/e$ its value at the interface. The magnitude of the electric field at the interface also depends on the angle of incidence, θ .

As a result of the evanescent wave, light propagating in a waveguide can excite probe molecules that are located within a distance from the interface approximately equal to the penetration depth. This distance is of the order of 100nm and according to equation 2 depends on the wavelength of the exciting radiation, the refractive indices of the waveguide and the medium, and the angle of incidence that the propagating light makes at the waveguide/medium interface. The probability of excitation depends on the electric field amplitude and therefore falls off exponentially away from the surface. For this reason, evanescent wave excited fluorescence samples the interfacial region, in contrast to the distal-type sensor design.

EXPERIMENTAL STUDIES

Experiments were conducted to investigate factors that may affect or limit the usefulness of optic fibers in cure monitoring systems. One potential advantage of the waveguide-type sensor is that the fluorescence signal is generated along the entire length of the fiber, and therefore descriptive of the entire system. We have examined the dependence between the fluorescence signal and the length of fiber exposed to the medium. Another aspect investigated was the effect of the difference in the refractive indices of the optic fiber and surrounding medium on the fluorescence signal. In order for a fiber to operate as a waveguide, the refractive index of the fiber must be higher than that of the surrounding material. The penetration depth of the evanescent wave and the efficiency of the waveguide to collect the fluorescent light depend on the refractive index difference. In addition, the refractive index of the resin system is expected to change during cure as a result of changes in density and chemistry⁶. To explore the degree to which the observed fluorescence is affected by the refractive index difference, experiments were

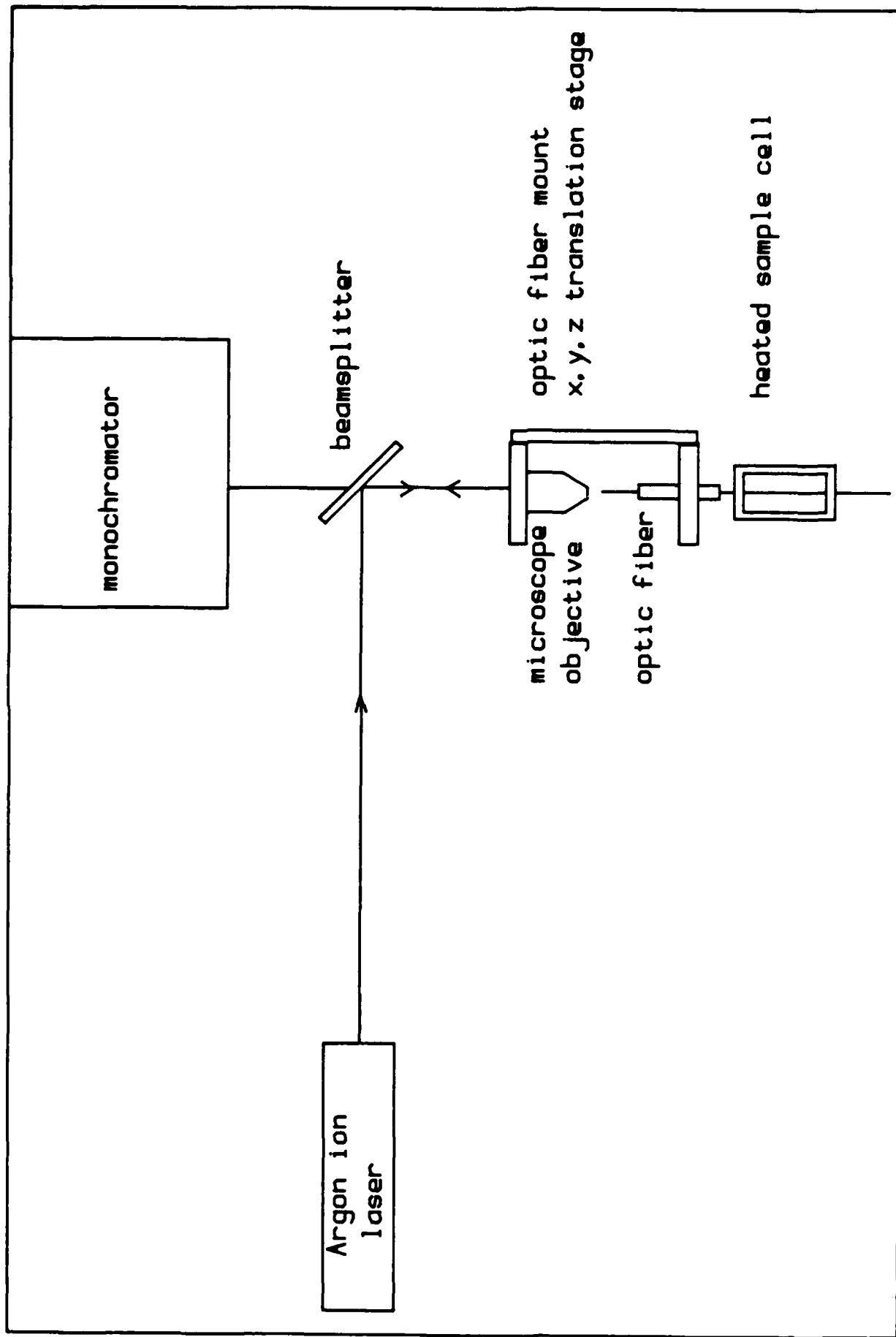


Fig. 9 Optical setup for measurement of fluorescence intensity using waveguide type optic fiber probes.

RHODAMINE B

SOLUTION B

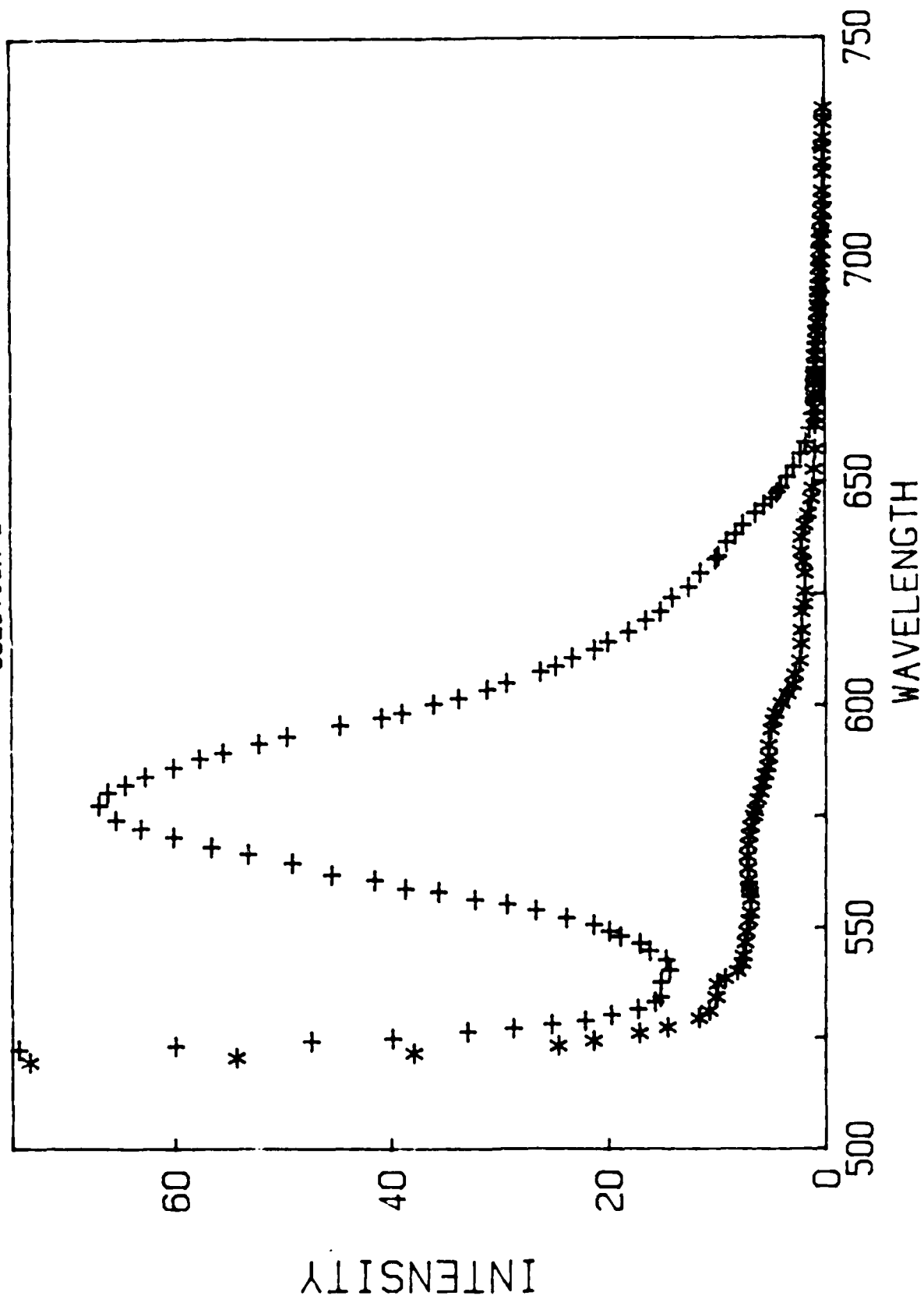


Fig. 10 Fluorescence spectrum of rhodamine-B in a solvent mixture of propanol-1 and dichlorobenzene obtained with waveguide type optic fiber (+), and fluorescence spectrum of optic fiber (*).

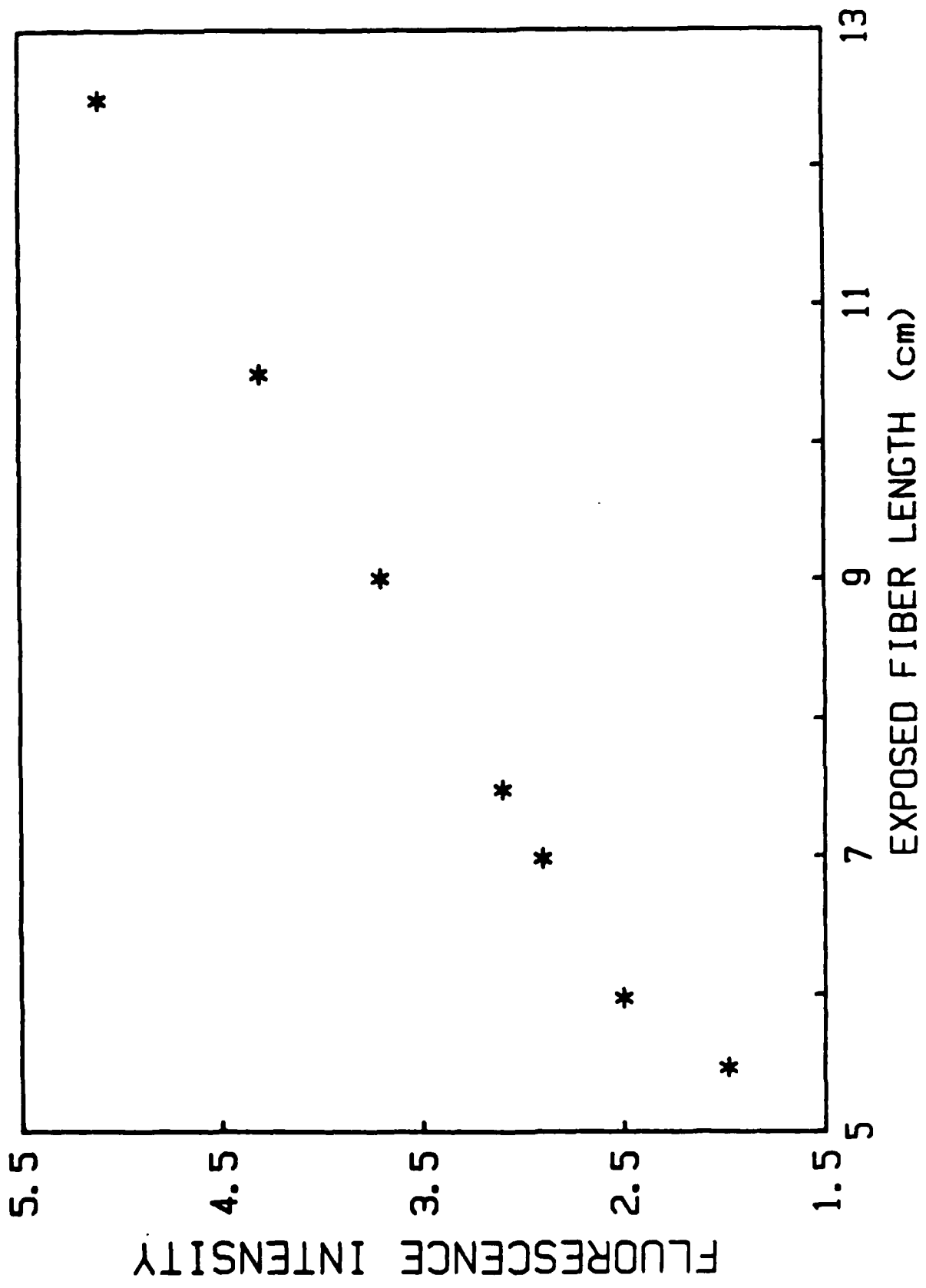


Fig. 11 Dependence of the fluorescent light intensity collected by a waveguide-type optic fiber sensor from a rhodamine-B solution on the length of fiber exposed to the dye solution.

conducted using dyes dissolved in mixtures of two solvents having different refractive indices.

All experiments were carried out using one of two setups, both of which simulated arrangements envisaged for real time cure monitoring. The setup diagrammed in figure 9 collects the fluorescence from the proximal end of the fiber, whereas in the other setup the fluorescence is collected at the distal end. In either arrangement, light from an argon ion laser is focussed onto one end (proximal) of the optic fiber. The fiber is held in a commercial fiber mount which can be adjusted to position the fiber at the focal point of the objective. The fiber, which is stripped of cladding, if any, passes through the sample. The fluorescence light is collected at the distal end of the fiber in one arrangement and in the other, as shown in figure 9, collected through a beamsplitter from the proximal end of the fiber. In either arrangement, the fluorescence light is focussed onto the entrance slit of a double 0.25M monochromator, and the intensity measured as a function of wavelength by photon counting electronics.

The dependence of the fluorescence signal on exposed fiber length was obtained for a 100 micrometer diameter waveguide made of ordinary silica, refractive index 1.46, and the dye rhodamine-B at a concentration of $10^{-5}M$ in a 30/70 by volume mixture of dichlorobenzene and propanol-1. The fluorescence spectrum of rhodamine-B obtained with excitation at 488nm is shown in figure 10, and the peak intensity as a function of the length of fiber exposed to the solution is depicted in figure 11. The findings given in figure 11 show a linear relationship between fiber length and fluorescence intensity. In these experiments, no attempt was made to optimize the fluorescence signal so that the minimum length of fiber needed to obtain good quality data has not been

FLUORESCENCE MONITORING USING OPTIC FIBERS

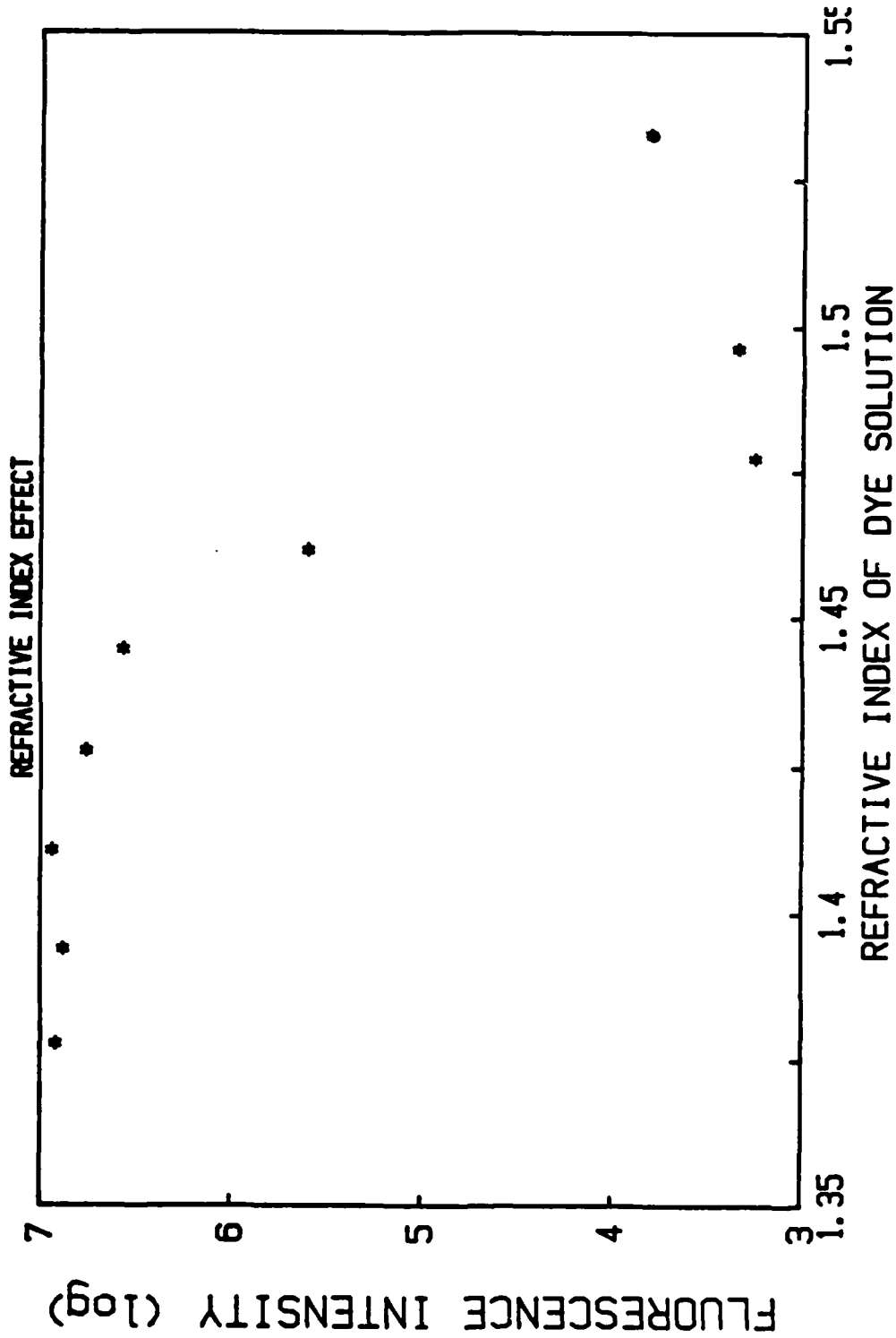


Fig. 12 Dependence of the intensity of fluorescent light from rhodamine-B solutions collected by optic fiber (index 1.46) on the solvent refractive index.

addressed. Other factors such as the total change in fluorescence intensity during a cure cycle, fiber characteristics (diameter, refractive index composition), laser intensity, and dye concentration will influence the minimum length of exposed fiber required for measurement of state of cure.

The straight line of figure 11 extrapolates to the origin, zero intensity at zero length, which provides an internal check on the data. This observation differs from that made by Andrade et al²⁸ who used a somewhat similar design to determine fluorescence from solutions. In their optic fiber system, the fiber terminates in the solution; the distal end is blackened, and the signal is observed from the proximal end of the fiber. With this design, their plot of signal intensity versus immersion depth does not extrapolate to zero intensity, but to a finite value. A possible explanation is that guided light may escape the fiber at the air-solution interface and excite molecules situated outside the fiber-solution interfacial region. Light will escape the fiber at the air-solution boundary because the critical angle for fiber/air is less than that for fiber/solution owing to the difference in refractive index between air and the solution. With proper selection of the optics coupling the laser beam into the fiber, the effect can be minimized as demonstrated by the data shown in figure 11.

Experiments also verified that a linear relationship existed between the dye concentration and the fluorescence intensity.

As the refractive indices of epoxies are in the range 1.5-1.6 one potential problem is the availability of fibers of high refractive index. It is likely that the fiber index would have to be close to that of the resin. For this reason, we have examined the dependence of the fluorescence intensity observed with a fiber on the difference between refractive indices of the

waveguide and surrounding medium. In figure 12 is shown the fluorescence intensities observed with a glass fiber (index 1.46) immersed in rhodamine-B solutions of different refractive indices. Refractive indices in the range 1.34 to 1.56 were obtained with mixtures of propanol-1 and dichlorobenzene. Care was taken to ensure that the same length of fiber was exposed to the solution for each measurement. The observed fluorescence increases by three orders of magnitude when the solution refractive index is less than that of the glass fiber. The residual intensity observed with the solution index higher than that of the fiber is attributed to scattering of the propagating light at the air-liquid interface. The scattering results from a change in the minimum angle of incidence for total internal reflection when the surrounding medium refractive index increases at the air-liquid interface. The observed fluorescence intensities are also sensitive to the effects of the refractive index mismatch on the efficiency of the fiber to collect some of the fluorescence light for transmission through the fiber to the detector. The effects of the refractive index and fiber diameter on the collection efficiency has been analyzed theoretically and will be discussed in the next section.

The dye systems described in the preceding section require excitation in the near UV and UV regions of the electromagnetic spectrum. Unfortunately, most glasses, particularly those with refractive indices higher than that of epoxy resins, fluoresce strongly upon excitation by radiation in this wavelength range. Optic fibers made of high purity quartz have been used to excite and collect fluorescence of probe molecules which have been excited at 363.8nm by an argon laser with UV reflectors. However, the refractive index of quartz is too low for use as a waveguide with epoxy resins. Owing to the limitations of glass fibers we have explored the potential of plastic fibers made of

polystyrene, PS, and poly(methyl methacrylate), PMMA. The refractive index of PS is 1.6 and PMMA has an index of 1.499. The latter material, PMMA, may be marginally acceptable for some epoxy systems, whereas the former has general application. Both plastic fibers are chemically inert in an epoxy system. Another possibility, which may be worthy of consideration, is the fabrication of optic fibers from epoxy resins. This is attractive for the following reasons. The refractive index of the epoxy fiber would be higher than that of the epoxy prepolymer resin because of densification, and subsequent to cure the fiber would have a chemical composition very similar to that of the cured resin. The latter effect could be important if the optic fibers made of glass serve as failure initiation sites when the composite parts in which they are imbedded are placed in service.

THEORETICAL CONSIDERATIONS

It is desirable to improve the efficiency of fiber optics fluorescence excitation and collection systems in order to reduce fiber diameters and probe concentrations, as well as to permit the use of less expensive light sources and detection systems. Efficiency, as used here, is defined as the product of the probabilities of fluorescence excitation with evanescent wave light and of observing a photon of fluorescent light at the detector end of the optic waveguide. Calculations were conducted to determine the effect of various factors, listed in Table 1, on the excitation and collection probabilities. In addition to the factors listed in Table 1, we considered the effect of the probe molecule absorption on the refractive index of the resin-probe medium and we will discuss this aspect first.

As evident from figure 12, small changes in the refractive index of the epoxy-probe system when the waveguide index is only slightly larger can have a

demonstrable effect on the waveguide excitation and collection efficiency. The high refractive index of epoxies relative to most waveguide materials is likely to limit the available range of refractive index differences between the waveguide and medium. It is possible, therefore, that the medium index would be only slightly less than that of the fiber waveguide and the effect of the dye on the refractive index should be considered. Although the probe concentration is low its effect on the medium refractive index at the excitation and emission wavelengths may be non-negligible owing to anomalous dispersion.

Dispersion in the refractive index, n_m , in the frequency range of the probe absorption was modeled by the Lorenz-Lorentz relation³²,

$$n_m^2 = n_0^2 + 4\pi N e^2 f (\omega'^2 - \omega^2) / m_e [(\omega'^2 - \omega^2) + \gamma^2 \omega^2] \quad [3]$$

In this equation, n_0 is the refractive index of the epoxy without the probe, N is the probe concentration in number of molecules per cc, e and m_e are the charge and mass of the electron, ω is the frequency of the light, γ and f are the halfwidth and oscillator strength of the electronic transition, respectively, and ω' is the electronic transition frequency shifted by $-4\pi e^2 f / 3 m_e$. The frequency dependence of the refractive index given by equation 3 has implications for both the excitation and collection of fluorescent light by an optic fiber. The presence of the probe molecule has no effect on the refractive index for $\omega = \omega'$, increases the refractive index above n_0 for $\omega < \omega'$, and lowers the refractive index below n_0 at frequencies greater than ω' .

Based on equation 3 it may be possible to select an excitation frequency greater than ω' thereby decreasing the refractive index of the medium. Unfortunately, the few laser lines available and the low probability of

electronic excitation off-resonance militate against achieving a lower refractive index through the presence of the absorbing probe. In the case of the emission, the refractive index of the epoxy and probe system would be greater than that of the epoxy alone since the fluorescence frequencies are less than ω' .

We calculated the maximum change in refractive index to be 0.01 using a probe concentration of 10^{-4} mol/l, a frequency ω' corresponding to 500nm, an oscillator strength, f , of 1.0, and a bandwidth, γ , of 2000cm^{-1} . Reference to figure 12 shows that a change of this magnitude would only affect the efficiency of the optic fiber sensor if the difference in the refractive indices of the fiber and epoxy resin was less than 0.04.

TABLE 1

Input Parameters for Modeling Fluorescent Light Excitation
and Collection Efficiency of Optic Fibers

ELEMENT	PARAMETERS
laser source	frequency, beam profile and diameter
optic system	numerical aperture and power of objective lens used to focus laser light onto fiber
optical fiber	diameter and refractive index
medium	refractive index, quantum efficiency and concentration of probe

The calculation of the efficiency of the optic fiber excitation and collection can be divided into five parts:

(1) The intensity profile of the focussed laser beam as a function of the angle of incidence at the front (proximal) surface of the optic fiber; (2) the evanescent wave amplitude as a function of the angle of incidence at the

waveguide-medium interface and distance from the waveguide surface; (3) probability of absorption by probe molecule with photon emission; (4) portion of the fluorescent light entering the waveguide as a function of the angle of incidence at the medium/waveguide interface; and (5) transmission efficiency of the collected light. We will outline the computational approach to each of these 5 parts below.

The excitation and collection efficiency is given by the probability of observing a photon of fluorescent light at the end of an optic fiber collection system. The probability is given by

$$P(\lambda_o) = \pi \rho_o^2 C_o p(\lambda_o, \lambda') \int_0^L \int_0^{\pi/2} \int_0^\infty f(\theta_r) I(\theta_r, z, \lambda_o, n_m, n_g) d\theta_r$$

$$\int_0^{\pi/2} \int_0^{\sin^{-1}(\rho_o/(\rho_o+z))} \int_0^{\sin^{-1}(\rho_o/(\rho_o+z))} \sin(\phi) F_i(z, \phi, \psi, n_m, n_g) [F_r(z, \phi, \psi, n_m, n_g)] N(\phi, \psi, L-l) dz d\phi d\psi dl$$

[4]

The integration variables of equation 4 are defined as follows: θ_r is the angle of incidence of the excitation laser at the waveguide-medium interface; l is the axial fiber distance measured from where the optic fiber enters the sample and L is total length of fiber exposed to the medium; z is the radial distance measured from the fiber surface; ϕ and ψ are the angles of a spherical coordinate system located on the fluorescing molecule and their integration limits are set to include all emitted light rays that intersect the waveguide. Since the fiber optic illumination and detection system has radial symmetry, the integration over this angle variable is included in the factor multiplying the integral term. The remaining quantities of equation 4 which determine the excitation probability are as follows: C_o is the probe concentration; $p(\lambda_o, \lambda')$ is the probability of absorption of a photon of energy

hc/λ_0 with the emission of light of wavelength λ' ; $f(\theta_r)$ is the portion of the laser light beam intersecting the waveguide-medium interface at the angle θ_r ; and $I(\theta_r, z, \lambda_0, n_m, n_g)$ is the intensity of the evanescent wave at the radial distance z from the waveguide. The collection probability is given by the product

$$F_i(z, \phi, \psi, n_m, n_g) F_r(z, \phi, \psi, n_m, n_g)^{N(\phi, \psi, L-l)}$$

which gives the probability that a photon emitted at z, l in the direction ϕ, ψ arrives at the detector end of the optic fiber. $F_i(z, \phi, \psi, n_m, n_g)$ gives the fraction of light refracted into the fiber and $F_r(z, \phi, \psi, n_m, n_g)^{N(\phi, \psi, L-l)}$ is the portion of that light which reaches the detector. The exact form of F_i and F_r depends on whether the emitted light is evanescent as will be discussed below.

The computational approaches used in each of the previously mentioned five parts are defined as follows:

1. In our experiments, we used the 363.8nm UV line of an argon ion laser and a 20X, 0.4 NA microscope objective lens to focus the laser light onto the proximal face of the fiber. From the characteristics of the lens, the laser beam profile (Gaussian), and the beam diameter ($1/e^2$ intensity values) we determine the distribution of the incident light intensity, $g(\bar{\phi})$, as a function of the angle of incidence on the proximal fiber face. The distribution of the source intensity as a function of the angle of incidence, $f(\theta_r)$, at the waveguide-medium interface is found using Snell's law. The intensity distributions are related

$$f(\theta_r) = g(\bar{\phi}) \quad [5]$$

where

$$\bar{\phi} = \sin^{-1}(n_g \cos(\theta_r))$$

and the index of air is taken to be unity. Since only guided waves are of

interest, we limit consideration to angles of incidence at the waveguide proximal face that satisfy total internal reflection at the waveguide-medium interface, or

$$\bar{\phi} < \sin^{-1}((n_g^2 - n_m^2)^{1/2}) \quad [6]$$

The maximum value of $\bar{\phi}$ is limited by the numerical aperture of the focussing lens which can be selected to satisfy equation 6 and thereby to minimize light loss at the air-fiber-medium interface.

2. The amplitude of the evanescent wave at the distance z from the waveguide/medium interface is given by

$$\exp\left[-\frac{2\pi z n_g}{\lambda_0} (\sin^2(\theta_r) - (n_m/n_g)^2)^{1/2}\right] \quad [7]$$

where λ_0 is the wavelength of the excitation light in vacuum. The intensity is proportional to the square of the product of this quantity and $2 \cos(\theta_r)/(1 - (n_m/n_g)^2)^{1/2}$; the latter expression gives the functional dependence of the electric field at the interface on the angle of incidence and the refractive indices. In equation 1, the intensity form $I(\theta_r, z, \lambda_0, n_m, n_g)$, is

$$I(\theta_r, z, \lambda_0, n_m, n_g) = \frac{4 \cos^2 \theta_r}{(1 - (n_m/n_g)^2)} \exp\left[-\frac{4\pi z n_g}{\lambda_0} (\sin^2(\theta_r) - (n_m/n_g)^2)^{1/2}\right] \quad [8]$$

This expression is plotted in figure 13 as a function of the angle of incidence, θ_r and distance, z .

3. The probability of a molecule emitting a photon at wavelength λ' is given by the sum of the probabilities of spontaneous and stimulated emission, with

EVANESCENT WAVE SPECTROSCOPY

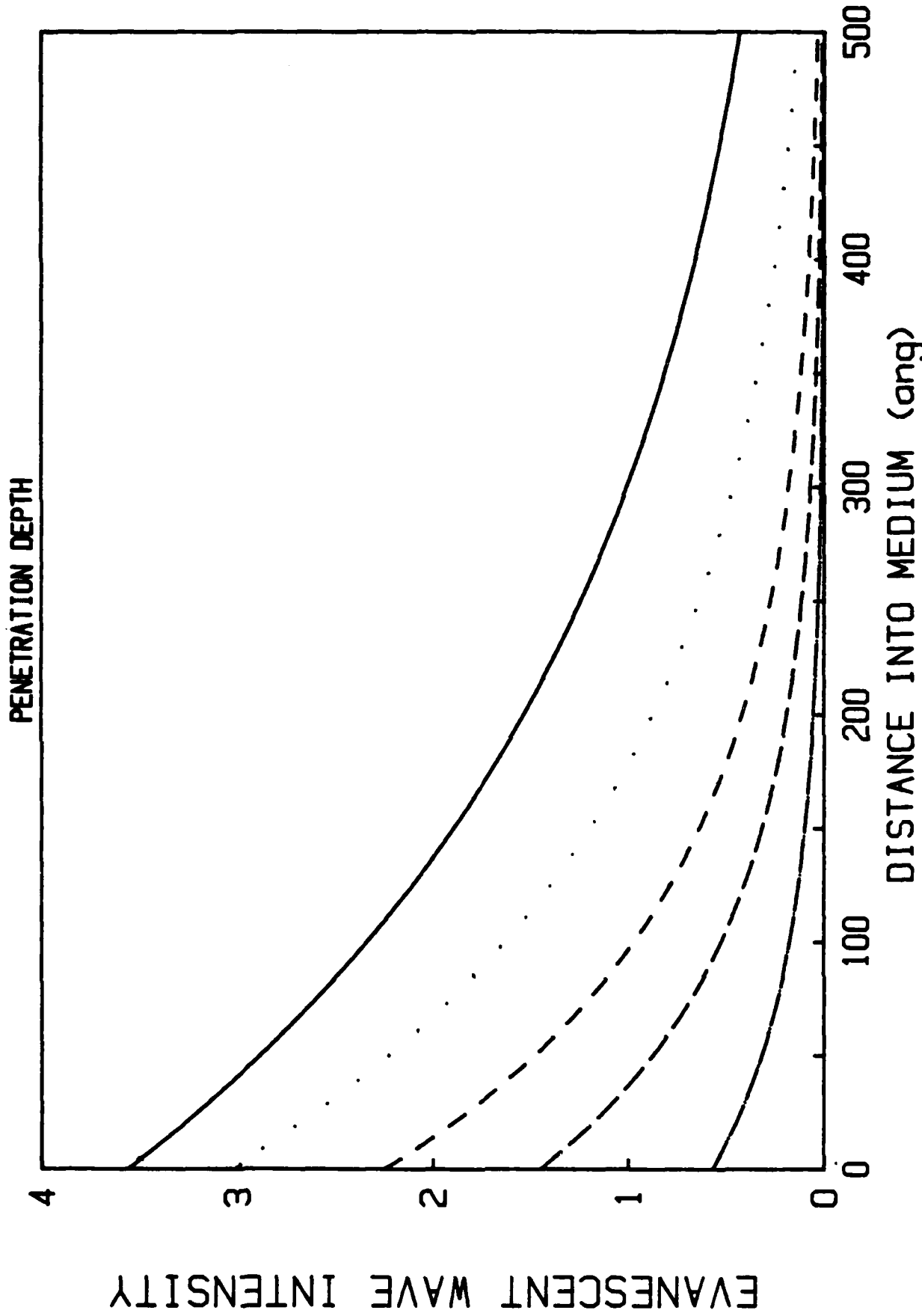


Fig. 13 Evanescent wave amplitude as functions of distance into lower refractive index medium and angle of incidence at the fiber-medium interface.

the latter proportional to the energy density of radiation of the wavelength λ' .

$$p(\lambda') = \frac{e^2 f \lambda' E^2}{4h m_e C} + \frac{8\pi^2 e^2 f}{C^2 m_e \lambda'} \quad [9]$$

where e , m_e are the charge and mass of the electron, respectively; C is the velocity of light; h is Planck's constant; f is the oscillator strength of the electronic transition; λ' is the wavelength of emission; and E is the electric field amplitude at the molecule. Alternately, the probability of fluorescence may be expressed as the product of the quantum efficiency, \bar{q} and the probability of absorption. The quantum efficiency is defined as the probability that an excited molecule will emit light to return to the ground state rather than take non-radiative pathways to electronic de-excitation. The variation in the quantity \bar{q} with medium viscosity gives the sensitivity of the fluorescence method for viscosity monitoring.

4. A probe molecule situated at the distance z from the interface will fluoresce with the probability $p(\lambda_0, \lambda') I(\theta_r, z, \lambda_0, n_m, n_g)$. Not all of the fluorescent light will impinge on the detector. To determine the solid angle intercepted by the fiber we treat the fluorescing molecule as a point source at z and determine the angles of incidence that the wavefront normals make with the fiber surface normal. This angle is given by

$$\theta_s = \sin^{-1} \left\{ \frac{\sin(\phi)}{z} [\rho^2 \cos(\psi) - \rho^2 + z^2]^{1/2} \right\} \quad [10]$$

where $\rho = \rho_0 + z$, and ϕ , ψ are the angles of a spherical coordinate system situated on the fluorescing molecule at z . The \bar{z} axis of the spherical

OPTIC FIBER SENSOR

COLLECTION EFFICIENCY

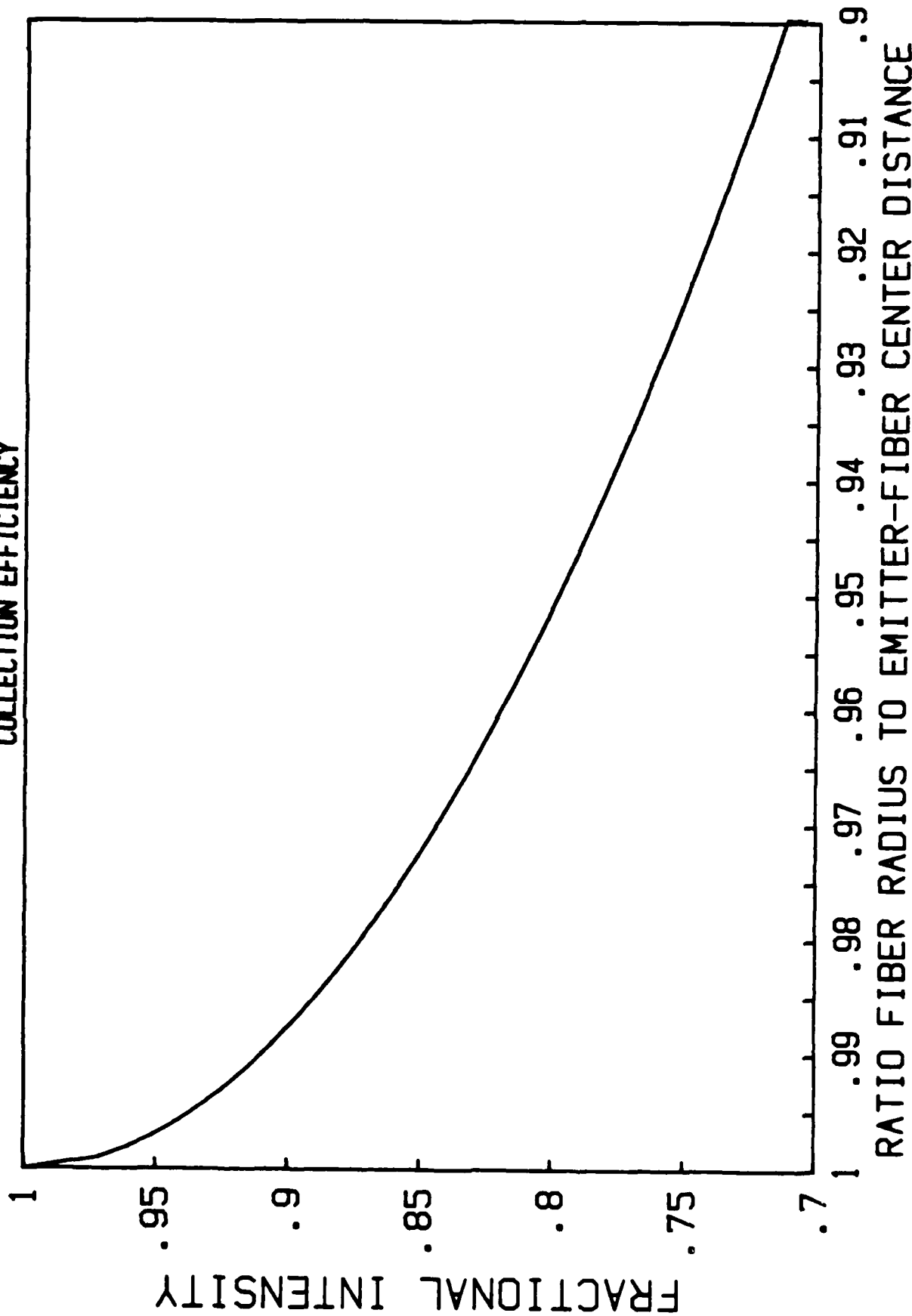


Fig. 14 Fraction of fluorescent light incident on optic fiber as function of the ratio of fiber radius to distance between emitter and fiber center.

coordinate system is parallel to the optic fiber direction, l (of equation 4), and ϕ is the angle between \bar{z} and the wavefront normal. To include all light refracted into the fiber which would propagate in the positive l direction, ϕ varies between 0 and $\Pi/2$ and ψ between $-\sin^{-1}(\rho_0/\rho)$ and $\sin^{-1}(\rho_0/\rho)$.

Figure 14 shows the fraction of light incident on the fiber as a function of the fiber radius and distance from the fiber surface. Departures from the optimal value exist only for exceedingly small fiber diameters and/or large distances. For distances over which the amplitude of the evanescent wave is significant ($0 < z < \lambda_0$) $z/\rho \ll 1$ since ρ_0 is typically in the range 25-100 μm and $\lambda_0 \sim 500\text{nm}$. This implies that approximately 1/2 of the light emanating from the point z impinges on the optic fiber.

5. Some of the fluorescent light incident on the optic fiber at the angle of incidence θ_s , given by equation 10, will be refracted into the fiber and propagate down the fiber to the detector. The efficiency of the collection and transmission depends on whether the angle θ_s is greater or less than the critical angle,

$$\theta_{s,c} = \sin^{-1}(n_m/n_g) \quad [11]$$

All the refracted light for $\theta_s > \theta_{s,c}$ and propagating towards the detector will reach the detector end of the fiber unless losses occur through scattering from voids, impurities, etc. Light refracted into the fiber at angles of incidence less than the critical angle propagates towards the detector by successive reflections at the waveguide-medium interface, but with intensity loss at each reflection owing to refraction into the medium.

The principle of reciprocity in electromagnetic theory leads to the prediction that emission from an evanescent wave excited molecule, located near

the interface, should give rise to a totally internally reflected wave in the waveguide³³. The results given in reference 19 and in figure 11 are experimental verification of this prediction for the following reasons. If the fluorescing molecule is treated as a point source, e.g., the molecule is situated far from the interface, it is easily shown that no light would be refracted into the fiber such that it has an angle of incidence with the waveguide-medium interface greater than the critical angle, $\sin^{-1}(n_m/n_g)$. A consequence is that light entering the waveguide would not undergo total internal reflection and a portion of the fluorescent light would escape the waveguide because of refraction. Except near the critical angle, the loss through refraction at each reflection would be high and owing to the large number of successive reflections needed to propagate the light to the detector, virtually no fluorescence would reach the detector. If no fluorescent light propagates in the waveguide at angles of incidence greater than the critical angle then only light that enters the fiber near the detector would have a high probability of reaching the detector. As a consequence, the detector signal would not depend linearly on the length of the fiber exposed to the medium but would increase rapidly at lengths of the order of the fiber diameter and plateau at longer lengths. The observed linear dependence of the fluorescence signal with exposed fiber length as well as the observation of light entering the waveguide at angles beyond the critical angle support the notion of the emission of evanescent waves by excited molecules.

The theory of the emission of evanescent waves by excited molecules has been treated by Carniglia, et al³³ and Lukost and Kunz³⁴ using a classical treatment of the transition dipoles. We will outline the treatment of Carniglia, et al³³ and expand on it as necessary for the system under

consideration here. We seek the electric field amplitude in the waveguide originating from a transition dipole, P situated a distance z from the waveguide-medium interface. Note that treatment of the excited molecule as a point source leads to the result that fluorescent light refracted into the waveguide cannot propagate at angles of incidence (with the normal to the waveguide-medium interface) greater than the critical angle. The presence of a wave propagating in the waveguide in a direction beyond the critical angle would imply the emission of an evanescent photon. Whereas Carniglia et al³³ treated a transition dipole oriented in a plane parallel to the interface we will use a transition dipole with random orientation, and then average over all orientations. The treatment of a dipole oriented perpendicular to the interface is presented in reference³⁴. Let p_1, p_2, p_3 be the projections of the transition dipole on three mutually perpendicular directions corresponding to the radial(z) and axial(x) fiber directions with the third direction mutually perpendicular to these two. The electric field on the surface of the waveguide ($z=0$) is given in the plane wave spectrum representation as

$$E(x, y, 0, t) = \frac{-i}{2\pi} \int_{-\infty}^{\infty} \int_{-\infty}^{\infty} dK_1 dK_2 \frac{\exp(iK_3 z)}{K_3} [(K \cdot P)K - K^2 P] \exp i(K_1 x + K_2 y - Kt) \quad [12]$$

where K is the wavevector in the medium with components, K_1, K_2, K_3 and K is the angular frequency in units such that the velocity of light in vacuum is $C=1$.

The plane wave expression for the electric field across a dielectric boundary and originating from an oscillating dipole has been solved numerically³⁵ for various values of rK where r is the distance from the observation point to the dipole. The range of rK in the calculation³⁵ included both the near and far field limits. The treatment in reference 34 is in the near field limit. Both limits lead to identical expressions for the angular

distribution of intensity and dependence on the distance from the interface.

An analytical solution to equation 12 has been obtained in the far field limit³³ which has the advantage that the functional dependence of the intensity on the observation angle, the refractive index ratio, and the distance between the dipole and the interface can be shown. We will use a similar approach in our treatment of radiation from a randomly oriented dipole in the far field limit.

The term $[(\mathbf{P} \cdot \mathbf{K})\mathbf{K} - K^2\mathbf{P}]$ is decomposed into the TE and TM components

$$(\mathbf{P} \cdot \mathbf{K})\mathbf{K} - K^2\mathbf{P} = P_0 [\alpha\epsilon + \beta (\hat{\mathbf{K}} \times \epsilon)] \quad [13]$$

where ϵ is the unit vector normal to \mathbf{K} and the plane of incidence, (TE), and $\hat{\mathbf{K}}$ is the unit wave vector, \mathbf{K}/K , so that $\hat{\mathbf{K}} \times \epsilon$ is the TM polarization. P_0 is the dipole moment magnitude,

$$P_0 = (p_1^2 + p_2^2 + p_3^2)^{1/2}$$

Expansion of equation 13 yields

$$\alpha = K^2 (p_2 K_1 - p_1 K_2) / (K_1^2 + K_2^2)^{1/2} \quad [14]$$

and

$$\beta = (K_1^2 + K_2^2)^{1/2} K (p_1 K_1 + p_2 K_2 + p_3 K_3) - K^3 (K_1 p_1 + K_2 p_2) / K_3 (K_1^2 + K_2^2)^{1/2} \quad [15]$$

The TM term differs from those of reference 33 in that p_3 components are present whereas the TE component is identical since TE is perpendicular to the interface, and hence to z . Using the Fresnel formulas³⁵ we have for the field in the waveguide,

$$\mathbf{E}(\mathbf{r}, t) = \frac{-iP_0}{2\pi} \int_{-\infty}^{\infty} \int_{-\infty}^{\infty} dk_1 dk_2 \exp(iK_3 z) \left[\frac{2\alpha\epsilon}{k_3 + K_3} + \frac{2n\beta(K \times \epsilon)}{k_3 + n^2 K_3} \right] \quad [16]$$

where n is the refractive index ratio, n_g/n_m . Equation 16 is solved in the far-field limit to yield

$$E(R,T) = \frac{P_0}{R} \exp(iK_3 z) \left[\frac{2\alpha k_3}{k_3 + K_3} \epsilon + \frac{2n\beta k_3}{k_3 + n^2 K_3} (K \times \epsilon) \exp i(nK \cdot R - Kt) \right] \quad [17]$$

The k values now correspond to directions along r , the other components being negligible in the far field approximation.

The intensity of light for the TE mode at the interface but inside the waveguide and propagating in the direction θ_s measured from the interface normal becomes

$$I(\theta_s, R) = \frac{P_0^2}{R^2} \frac{4\alpha^2 k_3^2}{(k_3 + K_3)^2} \quad [18]$$

for $\theta_s < \theta_{sc}$ and

$$I(\theta_s, R) = \frac{P_0^2}{R^2} \frac{4\alpha^2 k_3^2}{k_3^2 + |K_3|^2} \exp(-2|K_3|z) \quad [19]$$

for $\theta_s > \theta_{sc}$

Let θ_s' be the angle of incidence in the lower index medium so that

$$k_3 = n_g K \cos(\theta_s) \quad [20a]$$

and

$$K_3 = n_m K \cos(\theta_s') \quad [20b]$$

The angles θ_s and θ_s' are related by $\theta_s' = \sin^{-1}(n_g/n_m \sin \theta_s)$,

$$\text{or } |K_3| = n_m K (n_g^2/n_m^2 \sin^2(\theta_s) - 1)^{1/2} \quad \theta_s' > \theta_{sc} \quad [21]$$

Substituting equations 20 and 21 into equation 18 we have

$$I(\theta_s, R) = \frac{4P_0^2 \alpha^2 \cos^2 \theta_s \sin^2 \theta_s'}{R^2 \sin^2(\theta_s + \theta_s')} \quad [22]$$

and equation 19 becomes

$$I(\theta_s, R) = \frac{P_0^2 4\alpha^2 \cos^2(\theta_s)}{R^2 (1 - n_m^2/n_g^2)} \exp\left(-\frac{4\pi z n_g}{\lambda_0} (\sin^2(\theta_s) - n_m^2/n_g^2)^{1/2}\right) \quad [23]$$

Integration of α^2 , where α is given by equation 12, over all orientations of the transition dipole moment yields

$$\langle \alpha^2 \rangle = \frac{4K^4 P_0 \Pi}{3}$$

ANGULAR DISTRIBUTION

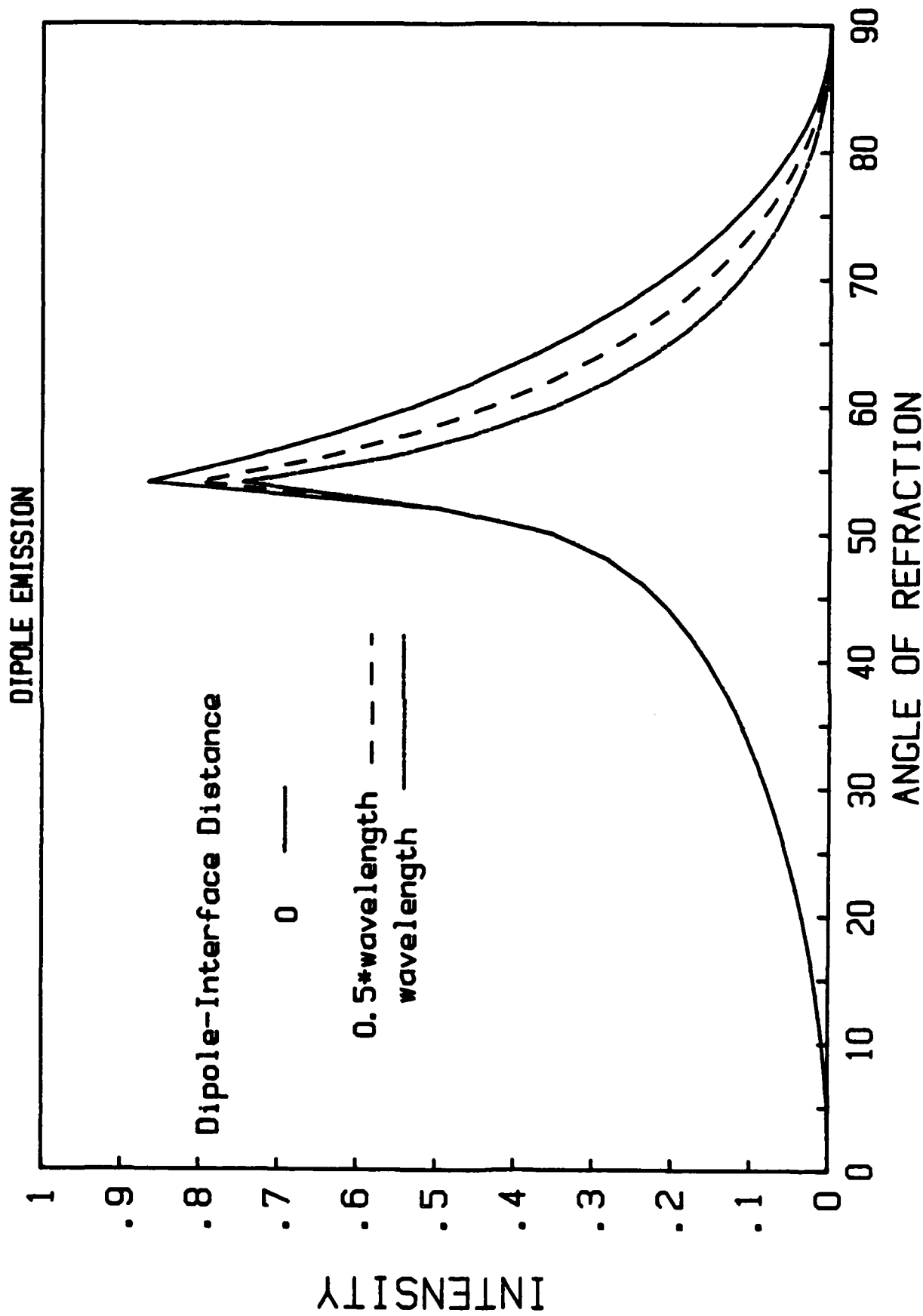


Fig. 15 Angular distribution of transition dipole's emission with angle measured from transition moment axis. The critical angle is 54° .

The expression 23 differs from equation 22 by the exponential term $\exp(-2z|K_3|)$ which is identical in form to the evanescent wave decay. Thus, the signal at the detector depends exponentially on the distance between the fluorescing molecule and the fiber surface in the probabilities of both the excitation and collection of fluorescent light. For this reason, the evanescent wave type of sensor is particularly sensitive to the interface region.

When $\theta_s' > \theta_{sc}$ equation 23 replaces the term $F_i * F_r^{N(\phi, \psi, L-l)}$ of equation 4 for the TE polarization. The TM mode contribution is determined in a similar manner using the β expression. In figure 15 we show the angular distribution of the fluorescent intensity observed in the waveguide and originating from a dipole situated in the lower index medium. The maximum intensity occurs at the critical angle determined by the refractive index ratio. The intensity at angles greater than the critical angle derives from evanescent wave emission and propagates without loss to the detector. Light which enters the waveguide at angles less than the critical angle decays in intensity rapidly as it propagates down the waveguide owing to losses by refraction. The different curves of figure 15 give the dependence of the emitted intensity observed in the waveguide on the distance between the dipole and the waveguide interface. Inserting equation 23 for the terms $F_i(z, \phi, \psi, n_m, n_g) [F_r(z, \phi, \psi, n_m, n_g)]^{N(\phi, \psi, L-l)}$ in equation 4 we calculate the intensity distribution as a function of the refractive indices n_m and n_g . The calculated values for the refractive indices of the data shown in figure 12 are compared to the experimental values in figure 16. The calculated intensity was scaled to fit the experimental value in the plateau region, refractive index ratio > 1.04 . The agreement over the

EVANESCENT WAVE SENSOR

REFRACTIVE INDEX EFFECT

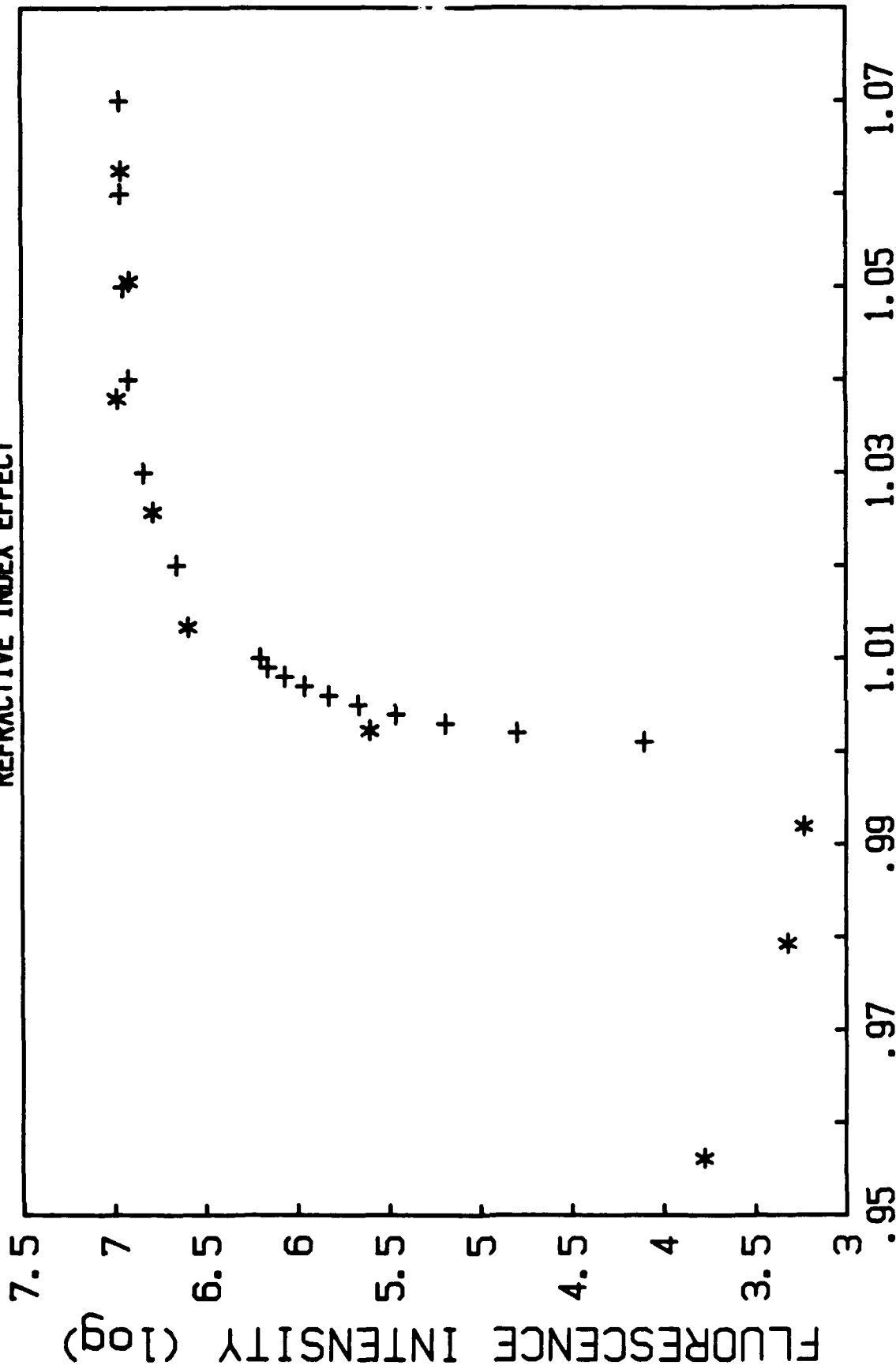


Fig. 16 Collection efficiency of optic fiber for evanescent wave emission θ_s as function of refractive index ratio; experimental points, +, calculated points, *.

range of refractive index ratio in which evanescent wave excitation occurs >1.0) is satisfactory.

We next consider the non-evanescent contribution to the fluorescent intensity collected and transmitted by the waveguide. The portion of light entering the fiber at the angle θ_s at the distance $L-l$ from the detector which reaches the detector is given by $F_r(\theta_s, n_m, n_g)^{N(\theta_s', L-l)}$ where $F_r(\theta_s, n_m, n_g)$ is the reflection coefficient at the fiber/medium interface averaged over the two polarizations:

$$F_r'' = \frac{\tan^2(\theta_s' - \theta_s)}{\tan^2(\theta_s' + \theta_s)} \quad [24a]$$

and

$$F_r^\perp = \frac{\sin^2(\theta_s' - \theta_s)}{\sin^2(\theta_s' + \theta_s)}; \quad [24b]$$

and $N(\theta_s', L-l)$ is the number of reflections necessary to propagate light which enters the fiber at the angle θ_s' with the interface normal the distance $L-l$,

$$N(\theta_s', L-l) = \frac{(L-l) \tan(\theta_s')}{2 \rho_o} \quad [25]$$

The functional dependence of the reflection and refraction coefficients with the angle of incidence θ_s is such that where the refracted light intensity is high (near unity), the reflection coefficient (at the opposite side of fiber interface) is low, and vice-versa. The refraction loss dominates the transmission efficiency, however, owing to the large number of reflection

required to propagate the fluorescence light down the fiber (see equation 25). The dominant contribution to the collected light intensity derives from the evanescent wave, for which $\theta_s \geq \theta_{sc}$.

REFERENCES

1. National Materials Advisory Board, "Materials for Lightweight Military Combat Vehicles", NMAB-396, National Research Council, Washington, D.C.(1982).
2. National Materials Advisory Board, "Organic Matrix Structural Composites: Quality Assurance and Reproducibility", NMAB-365, National Research Council, Washington, D. C.(1981).
3. Weatherhead, R. G., "FRP Technology Fibre Reinforced Resin Systems", Applied Science, London (1980).
4. Vinson, J. R., ed. "Advanced Composite Materials-Environmental Effects", STP 658, American Society for Testing and Materials, (1978).
5. Gillham, J. K., and Enns, J. B., J. Appl. Polym. Sci., 28, 2567(1983).
6. Tsai, S. W., and Hahn, H. T., "Introduction to Composite Materials", Technomic Publishing Co., Westport, CT(1980), Chap. 8.
7. Sanjana, Z.N., Polym. Eng. Sci., 26, 373(1986).
8. Bidstrup, W.W., Sheppard, N.F., Senturia, S.D., Polym. Eng. Sci. 26, 358 (1986).
9. Kranbuehl, D., Delos, S., Yi, E., Mayer, J. and Jarvie, T., Polym. Eng. Sci. 26, 338(1986).
10. Zukas, W. X., "Polymers and Polymer Matrix Composites Workshop", University of Connecticut, Storrs, CT., May, 1986.
11. Sung, C.S.P., Pynn, E. and Sun, H.-L., Macromolecules, 19, 2922(1986).
12. Levy, R. L., and Ames, D.P., in "Adhesive Chemistry Developments and Trends", L.-H. Lee, ed., Plenum Press, New York (1983).
13. Levy, R. L., Polym. Mater. Sci. Eng., 50, 124(1984).
14. Levy, R. L. and Ames, D.P., Polym Mater. Sci. Eng. 53, 176(1985).
15. Lakowicz, J., "Principles of Fluorescence Spectroscopy", Plenum Press, New York (1983), Chap. 7.
16. Wang, F. W., Lowry, R. E., and Fanconi, B., Polymer, 27, 1529(1986).

17. Fanconi, B., Wang, F. W., and Lowry, R. E., in "Review of Progress in Quantitative Nondestructive Evaluation", Plenum Press, New York, 6B, 1287(1987).
18. Wang, F. W., Lowry, R. E., Pummer, W. J., Fanconi, B., Wu, E.-S., ACS Symposium Series, in press.
19. Sung, C.S.P., Chin, I. J. and Wu, W.-C., *Macromolecules*, 13, 1570(1985).
20. Oster, G. and Nishijima, Y., *J. Am. Chem. Soc.*, 78, 1581(1956).
21. Birks, J. B., "Photophysics of Aromatic Molecules", Wiley Interscience, New York(1970).
22. Kauzmann, W., "Quantum Chemistry", Academic Press, New York(1957).
23. Law, K.Y., *Chem. Phys. Letrs.* 75, 545 (1980).
24. Fanconi, B., Wang, F., Hunston, D., Mopsik, F., "Cure Monitoring for Polymer Matrix Composites", in "Materials Characterization for Systems Performance and Reliability", J. W. McCauley and V. Weiss, eds., Plenum Press, New York,(1986).
25. Harrison, G. and Barlow, A. J., "Dynamic Viscosity Measurements", Vol. 19 pp 137-178, in "Methods of Experimental Physics", Academic Press, New York(1981).
26. Private communication, AT&T Laboratories.
27. Hirschfeld, T., Deaton, T., Milanovich, F., Klainer, S., *Opt. Eng.* 22, 527(1983).
28. Newby, K., Reichert, M. L., Van Wagenen, R., and Andrade, J. D., *Appl. Opt.* 23, 1812(1984).
29. Andrade, J. D., VanWagenen, R. A., Gregonis, D. E., Newby, K., Lin, J.-N., *IEEE Transactions on Electron Devices* Vol ED-32, 1175 (1985).
30. Newby, K., Andrade, J. D., Benner, R. E., and Reichert, W. M., *J. Coll. Interface Sci.*, 111, 280(1986).
31. Ditchburn, R. W., "Light", Interscience, New York(1963), Chap. 14.
32. *Ibid.*, Chap. 15.
33. Carniglia, C. K., Mandel, L., Drexhage, K. H., *J. Opt. Soc. Am.*, 62, 479(1972).

34. Lukosz, W. and Kunz, R.E., J. Opt. Soc.Am. 67, 1607 (1977) and ibid, pg 1615.
35. Burghart, T. P., and Thompson, N. L., Biophys. J., 46, 729(1984).
36. Born, W., and Wolf, E., "Principles of Optics", Pergamon Press LTD., London(1965), Chap. 1.

LIST OF PUBLICATIONS UNDER ARO SPONSORSHIP

"Picosecond Excimer Fluorescence Spectroscopy: Applications to Polymer-Segment Mobility and Polymerization Monitoring", F.W. Wang, R.E. Lowry and R.R. Cavanagh, *Polymer*, 26, 1657 (1985).

"Cure Monitoring of Epoxy Resins by Fluorescence Spectroscopy", F.W. Wang, R.E. Lowry, and B.M. Fanconi, *Polymeric Materials Science and Engineering*, 53, 180 (1985).

"Fluorescence Monitoring of Viscosity and Chemical Changes During Polymerization", F.W. Wang, R.E. Lowry, and B.M. Fanconi, *Polymer Preprints* 27 (2), 306 (1986).

"Cure Monitoring for Polymer Matrix Composites", B.M. Fanconi, F.W. Wang, D.L. Hunston, and F.I. Mopsik, in *Materials Characterization for Systems Performance and Reliability*, eds. J.W. McCauley and V. Weiss, Plenum Publishing, p. 275 (1986).

"Fluorescence Methods for Cure Monitoring of Epoxy Resins", F.W. Wang, R.E. Lowry, E.-S. Wu and B.M. Fanconi, *Proceedings of the 1985 Scientific Conference on Chemical Defense Research*, 573 (1986).

"Novel Fluorescence Method for Cure Monitoring of Epoxy Resins", F.W. Wang, R.E. Lowry and B.M. Fanconi, *Polymer*, 27, 1529 (1986).

"Process Monitoring of Polymer Matrix Composites Using Fluorescence Probes", B.M. Fanconi, F.W. Wang, and R.E. Lowry in *Review of Progress in Quantitative Nondestructive Evaluation*, eds. D.O. Thompson and D.E. Chimenti, Plenum Publishing, Vol. 6B, p. 1287 (1987).

"Comparisons Among Process Monitoring Techniques", B.M. Fanconi and F.W. Wang, *ANTEC '87*, 1100 (1987).

"In-Situ Characterization of the Interface of Glass Reinforced Composites", F.W. Wang and B.M. Fanconi, Final Report of ARO Contract MIPR ARO 111-84, NBSIR 870302 (1987).

"Cure Monitoring of Epoxy Resins by Fluorescence Recovery After Photobleaching", F.W. Wang and E.-S. Wu, *Polymer Communications*, 28, 73 (1987).

"Fluorescence Monitoring of Viscosity and Chemical Changes During Polymerization", F.W. Wang, R.E. Lowry, W. Pummer and B.M. Fanconi in "Photophysics of Polymer Systems" (J.M. Torkelson and C.E. Hoyle, eds.), ACS Symposium Series, in press.

"In-situ Fluorescence Monitoring of Viscosity and Chemical Changes During Processing of Polymer Composites", F.W. Wang, R.E. Lowry, and B.M. Fanconi, *Proceedings of the 1986 Scientific Conference on Chemical Defense Research*, in press.

END

11-87

DTIC